Engineering Applications of Artificial Intelligence 97 (2021) 104015

Contents lists available at ScienceDirect

Engineering Applications of Artificial Intelligence

journal homepage: www.elsevier.com/locate/engappai

Optimization of support vector machine through the use of metaheuristic algorithms in forecasting TBM advance rate

Jian Zhou [a,*], Yingui Qiu [a], Shuangli Zhu [a], Danial Jahed Armaghani [b,*], Chuanqi Li [a], Hoang Nguyen [c,d], Saffet Yagiz [e]

[a] School of Resources and Safety Engineering, Central South University, Changsha 410083, China
[b] Institute of Research and Development, Duy Tan University, Da Nang 550000, Viet Nam
[c] Department of Surface Mining, Mining Faculty, Hanoi University of Mining and Geology, 18 Vien st., Duc Thang ward, Bac Tu Liem dist., Hanoi, Viet Nam
[d] Center for Mining, Electro-Mechanical research, Hanoi University of Mining and Geology, 18 Vien st., Duc Thang ward, Bac Tu Liem dist., Hanoi, Viet Nam
[e] School of Mining and Geosciences, Nazarbayev University, 010000, Nur-Sultan city, Kazakhstan

ARTICLE INFO

Keywords:
TBM performance
Support vector machine
Whale optimization algorithm
Gray wolf optimization
Moth flame optimization

ABSTRACT

The advance rate (AR) of a tunnel boring machine (TBM) in hard rock condition is a key parameter for the successful accomplishment of a tunneling project, and the proper and reliable prediction of this parameter can lead to minimizing the risks associated to high capital costs and scheduling for such projects. This research aims at optimizing the hyper-parameters of the support vector machine (SVM) technique through the use of three optimization algorithms, namely, gray wolf optimization (GWO), whale optimization algorithm (WOA) and moth flame optimization (MFO), in forecasting TBM AR. In fact, the role of these optimization techniques is to optimize the hyperparameters 'C' and 'gamma' of the SVM model to get higher performance prediction. To develop the hybrid SVM-based models, 1,286 sample sets of data collected from a water transfer tunnel in Malaysia comprising seven input variables, i.e., rock mass rating, uniaxial compressive strength, Brazilian tensile strength, rock quality designation, weathering zone, thrust force and revolution per minute, and one output variable, i.e., TBM AR, were considered and used. Several GWO-SVM, WOA-SVM and MFO-SVM models were constructed to predict TBM AR considering their effective parameters. The accuracy levels of the proposed models were assessed using four statistical indices, i.e., the coefficient of determination (R^2), root mean squared error (RMSE), mean absolute error (MAE), and variance accounted for (VAF). Modeling results revealed that the MFO algorithm can capture better hyper-parameters of the SVM model in predicting TBM AR among all three hybrid models. R^2 of (0.9623 and 0.9724), RMSE of (0.1269 and 0.1155), and VAF of (96.24 and 97.34%), respectively, for training and test stages of the MFO-SVM model confirmed that this hybrid SVM model is a powerful and applicable technique addressing problems related to TBM performance with a high level of accuracy.

1. Introduction

Tunnel boring machines (TBMs) are gigantic tools widely used to construct tunnels in an economical and efficient way. When excavating, TBMs are generally extremely sensitive to conditions of rock mass throughout the path. In case the rock mass condition is unknown and there is not enough information, the operating parameters may be set improperly, which can lead to a decline in safety and efficiency of the whole operation (Armaghani et al., 2017; Yagiz, 2017; Liu et al., 2020a; Gao et al., 2020; Zhou et al., 2019f). It should be noted that the TBM performance needs to be carefully predicted in order to provide an effective plan for tunneling projects and also to adopt the best construction techniques (Xu et al., 2019; Zhou et al., 2020a,b). Such predictions need to be accurate enough to minimize the rate of common risk occurrence and the disadvantages that can appear during every tunneling project (e.g., high capital costs).

The models presented in the literature for predicting the TBM performance (e.g., penetration rate, PR, and advance rate, AR) can be classified into three groups (see Fig. 1): (1) empirical and theoretical models, which are typically designed on the basis of laboratory tests, field performance of TBMs, cutting forces, and rock properties (Graham, 1976; Snowdon et al., 1982; Bamford, 1984; Rostami, 1997; Yagiz, 2002); (2) statistical models, which work generally on the

* Corresponding authors.
E-mail addresses: csujzhou@hotmail.com, j.zhou@csu.edu.cn (J. Zhou), 195512085@csu.edu.cn (Y. Qiu), 195512078@csu.edu.cn (S. Zhu), danialjahedarmaghani@duytan.edu.vn (D.J. Armaghani), lichuanqi@csu.edu.cn (C. Li), nguyenhoang@humg.edu.vn (H. Nguyen), saffet.yagiz@nu.edu.kz (S. Yagiz).

https://doi.org/10.1016/j.engappai.2020.104015
Received 11 June 2020; Received in revised form 27 September 2020; Accepted 12 October 2020
Available online 6 November 2020
0952-1976/

Abbreviations

ANFIS	Adoptive neuro-fuzzy inference system
TBM	Tunnel boring machine
PR	Penetration rate
FS	Feature space
AR	Advance rate
ANN	Artificial Neural Network
PSO	Particle swarm optimization
UCS	Uniaxial compressive strength
AI	Artificial intelligence
ML	Machine learning
CSM	Colorado School of Mines
RQD	Rock quality designation
TFC	Trust force per cutter
RPM	Revolution per minute
WZ	Weathering zone
RMR	Rock mass rating
R^2	Coefficient of determination
NTNU	Norwegian University of Science and Technology
FPI	Field penetration index
RMSE	Root mean square error
α	Planes of weakness
SVR	Support vector regression
SVM	Support vector machine
ICA	Imperialism competitive algorithm
PSRWT	Pahang Selangor Raw Water Transfer
WOA	Whale optimization algorithm
GWO	Gray wolf optimization
MFO	Moth flame optimization
RBF	Radial basis function
VAF	Variance account for
MI	Mutual information
MAE	Mean absolute error
BTS	Brazilian tensile strength
GMDH	Group modeling of data handling

basis of mathematical rules (Gong and Zhao, 2009; Mahdevari et al., 2014); and (3) computational models whose system is on the basis of artificial intelligence (AI) and machine learning (ML) (Benardos and Kaliampakos, 2004; Simoes and Kim, 2006; Adoko et al., 2017; Koopialipoor et al., 2019), as tabulated in Table 1. With regard to the empirical and theoretical models, for instance, Ozdemir (1977) could successfully predict PR of TBM considering the results of full-scale laboratory cutting tests and many regression analyses. The Colorado School of Mines (CSM) model was the resultant model proposed based on these efforts. Note that CSM was then updated by Rostami (1997). The Norwegian University of Science and Technology (NTNU) introduced the NTNU model for the same purpose. To construct this popular model, numerous regression analyses were conducted on both driving parameters and rock mass parameters (Bruland, 1998). In another study, Hamidi et al. (2010) attempted to make an analysis on the relationships between the five most important parameters of the rock mass rating (RMR) system and the TBM field penetration index (FPI). They could find a correlation among three parameters: orientation of discontinuities, uniaxial compressive strength (UCS), and FPI. Their results were found to be helpful in predicting FPI. Moreover, three rock mass classifications, namely Q_{TBM}, geological strength index, and rock mass excavatability (Zhou et al., 2020b) were suggested to be applied to the TBM performance prediction (Bieniawski et al., 2006; Barton, 2000; Von Preinl et al., 2006; Benato and Oreste, 2015; Frough et al., 2015). In general, the empirical and theoretical models consider only a limited number of parameters; these models do not take into account various important working conditions and material features (Bruines, 1998). Consequently, it can be said that they are not accurate enough to be applied to the prediction of TBM parameters (Yagiz and Karahan, 2015; Benardos and Kaliampakos, 2004).

The models in the second group, namely the statistical models working on the basis of mathematical rules, have been implemented in the prediction of the TBM performance. Yagiz (2008) and Yagiz et al. (2009) developed linear and non-linear multiple regression equations, respectively, to estimate the PR of TBM with the use of the data gathered from 7.5 km of the Queens Water Tunnel constructed in the United States. The dependent parameters set in their models were peak slope index, Brazilian tensile strength (BTS), UCS, the distance between plane of weakness, and the angle between tunnel axis and the planes of weakness (α), and the independent variable was the TBM PR values. A number of relationships were developed by Hassanpour et al. (2011) with an acceptable precision level between FPI and various rock mass parameters such as rock quality designation (RQD), joint spacing, UCS, and basic RMR. Their findings revealed that an integrated form of RQD and UCS can achieve the optimum results regarding the FPI estimation. In another project, Rayatdust et al. (2012) gathered data from 6.3 km of the Alborz tunnel located in Iran for the aim of predicting TBM PR. The predictors they applied to their model were α, UCS, and volumetric joint count. They succeeded to introduce a linear multiple regression equation applicable to the estimation of TBM PR with a proper level of precision. On the other hand, according to Alvarez Grima and Verhoef (1999), statistical models cannot be always counted on as effective models for accurately describing nonlinear and complicated systems. In addition, these models generally deliver a poor performance in the presence of outliers and extreme values in the data used (Alvarez Grima et al., 2000).

The algorithms designed based on AI and ML (the third group) have been found to be successful in exploring the relationship between the factors that affect the TBM performance and the TBM performance parameters. Mahdevari et al. (2014) introduced a number of models applicable to the estimation of TBM PR using support vector regression (SVR). In the literature, some other techniques proposed for TBM PR prediction can be found, e.g., fuzzy logic (Okubo et al., 2003; Yagiz and Karahan, 2011; Minh et al., 2017), particle swarm optimization (PSO), artificial neural networks (ANNs), etc. Two hybridized models, i.e., PSO–ANN and imperialism competitive algorithm (ICA)-ANN, were developed by Armaghani et al. (2017, 2019) in order to predict TBM PR and TBM advance rate. Additionally, Salimi et al. (2016) made use of SVR and adaptive neuro-fuzzy inference system (ANFIS) models for the purpose of predicting TBM PR. SVR was found to be more successful than ANFIS regarding the achievement of the defined objective. In another project, a hybrid model was developed by Fattahi (2016) through the integration of ANFIS and fuzzy c-means clustering approach for the same aim. Koopialipoor et al. (2019) introduced a new approach based on AI, namely group modeling of data handling (GMDH). It was mainly aimed at accurate prediction of TBM PR. Armaghani et al. (2018) developed a gene expression programming equation as a way to accurately estimate TBM PR. Offering a promising flexibility level is the common feature of the AI- and ML-based models. Such feature significantly helps to determine solutions of higher reliability and accuracy to various problems that may arise in engineering and science fields. These models are especially effective when applied to highly complicated, nonlinear problems (Yagiz and Karahan, 2011).

The successful application of support vector machine (SVM) and its related hybrid models in solving various geotechnical problems has been reported by several researchers. In the area of blasting and its environmental issues, Khandelwal (2011), Shi et al. (2012), Rad et al. (2018), and Yu et al. (2019) developed SVM-based models to predict ground vibration, rock fragmentation, flyrock distance, and

Table 1
Recent works on TBM performance prediction using AI techniques.

Reference	Model	Input	Output	Description	R^2
Ghasemi et al. (2014)	FIS	DPW, UCS, BI, α	PR	Using 151 datasets	$R^2 = 0.89$
Gholamnejad and Tayarani (2010)	ANN	DPW, UCS, RQD	PR	Using 185 datasets	$R^2 = 0.94$
Benardos and Kaliampakos (2004)	ANN	N, RQD, UCS, RMR, overburden, permeability	AR	–	–
Simoes and Kim (2006)	FIS	RMR, RQD, machine diameter and groundwater inflow	U	Using data of three TBM projects	–
Alvarez Grima et al. (2000)	ANN, ANFIS	CFF, UCS, RPM, Dc, TPC geometry, rock mass properties	PR, AR	A database consisting 640 TBM projects	–
Yagiz and Karahan (2011)	PSO	UCS, BTS, BI, DPW, α	PR	Number of 151 datasets	$R^2 = 0.67$
Mikaeil et al. (2009)	FIS	DPW, UCS, BTS, α, PSI	PR	Using dataset presented by Yagiz (2008)	–
Yagiz et al. (2009)	ANN	DPW, UCS, BI, α	PR	Using 151 datasets	$R^2 = 0.9$
Eftekhari et al. (2010)	ANN	UCS, Rock Type, Qu, BTS, RQD, RMR, Thrust, Torque, Rs	PR	Using 10 km data excavated in Zagros tunnel, Iran	$R^2 = 0.69$
Gholami et al. (2012)	ANN	UCS, RQD, Js, Jc	PR	Data of 121 tunnel sections	$R^2 = 0.72$
Salimi and Esmaeili (2013)	ANN	PSI, UCS, BTS, DPW, α	PR	Data of 46 sections of the Karaj–Tehran tunnel	$R^2 = 0.83$
Torabi et al. (2013)	ANN	UCS, C, φ, υ	PR, U	Data of Tehran–Shomal highway project	$R^2_{PR} = 0.99$ $R^2_{U} = 0.99$
Yavari and Mahdavi (2005)	ANN	Dc, UCS, Qu, TPC, Rock Type	PR	Data of 251 sections of Gavshan tunnel, Iran	$R^2 = 0.82$
Oraee et al. (2012)	ANFIS	RQD, DPW, UCS	PR	Using 177 datasets obtained from two tunnel projects	$R^2 = 0.69$
Mahdevari et al. (2014)	SVR	UCS, BTS, BI, DPW, α, SE, TF, CP, CT	PR	150 data points pertaining to the Queens Water Tunnel, USA	$R^2 = 0.98$
Adoko et al. (2017)	Bayesian model	UCS, BI, α, DPW	PR	A database containing 151datasets	$R^2 = 0.93$
Zhou et al. (2018)	RF, Cubist	UCS, BTS, PSI, DPW, a	PR	Using 200 datasets from two tunnel projects	$R^2 = 0.63$
Armaghani et al. (2018)	Gene expression	UCS, BTS, RMR, RQD, WZ	PR	A database (1286 datasets in total)	$R^2 = 0.83$
Koopialipoor et al. (2019)	ANN, DNN	UCS, RQD, BTS, RMR, WZ	PR	Using 1286 datasets	$R^2 = 0.93$
Koopialipoor et al. (2020)	LSTM	TF, CT, CP, PLSI,	PR	Using 2570 datasets	–
Zhou et al. (2020a)	ANN, GP	UCS, RQD, BTS, RMR, TFC, RPM	AR	Using 1286 datasets	$R^2 = 0.92$
Zhou et al. (2020e)	XGBoost	UCS, RQD, BTS, RMR, WZ, TFC, RPM	AR	Using 1286 datasets	$R^2 = 0.98$

Nomenclature: distance between planes of weakness (DPW); rock brittleness (BI); the angle between plane of weakness and TBM-driven direction (α); rock quality designation (RQD); Overload factor (N); rock mass rating (RMR); rock mass weathering (RMW); core fracture frequency (CFF); revolution per minutes (RPM); water table surface (WTS); cutter diameter (Dc); thrust per cutter (TPC); particle swarm optimization (PSO); peak slope index (PSI); quartz percentage (Qu); rotational speed of TBM (Rs); joint spacing (Js); joint condition (Jc); cohesion (C); friction angle (φ); Poisson's ratio (υ); specific energy (SE); thrust force (TF); cutterhead power (CP); cutterhead torque (CT); extreme learning machine (ELM); point loading strength index (PLSI); Long Short-Term Memory (LSTM); Deep Neural Networks(DNN); Random Forests (RF) and genetic programming (GP).

blast-induced rock movement, respectively. In field of rock mechanics and tunneling, a SVM model was proposed by Zhou et al. (2012) for solving the rockburst problem. In addition, Ceryan et al. (2013) and Jahed Armaghani et al. (2020) used the advantages of SVM-based models for predicting tensile strength and brittleness index of the rock material, respectively. Li et al. (2016) assessed stability of the tunnel, developing a hybrid-based SVM model. In another study, Zhou et al. (2019a) estimated the energy consumption of cutter head drives in shield tunneling using a hybrid SVM technique. Zheng et al. (2020) applied this technique for solving the problem related to the liquefaction-induced uplift displacement of the tunnel. In the field of soil mechanics and foundation engineering, Zhou et al. (2017b) introduced a SVM model for analyzing safety risk in deep foundations. Lateral load capacity of piles was modeled and predicted by SVM in the study conducted by Samui and Kim (2013). Zhao and Yin (2009) proposed an SVM- based technique with PSO for identification of geomechanical parameters. Farfani et al. (2015) successfully indicated that the SVM model is able to predict the dynamic characteristics of the soil–structure systems. Bearing capacities of the shallow and deep foundations were effectively predicted by the SVM-based models in the studies carried out by Samui (2012) and Pal and Deswal (2008), respectively. Based on the above discussion, SVM is considered as a powerful and applicable technique that is able to positively solve geotechnical-related problems and due to that, the authors of this study decided to use several hybrid SVM-based models for solving the TBM performance problem. It is important to note that as far as the authors know the hybrid SVM-based models have not been applied and proposed in the field of TBM performance prediction.

In recent years, AI and ML predictive models have been widely used and proposed to estimate TBM performance parameters (mostly for TBM PR prediction). However, as mentioned before, the use and proposal of novel hybrid predictive models on the basis of the concept of an SVM model optimized by some powerful optimization techniques is missing in this field. Hence, the main contribution of the present research is to use and develop the new hybrid SVM-based models in predicting TBM performance, i.e., TBM AR. To do this, we decided to utilize three well-known, powerful and applicable optimization techniques, i.e., gray wolf optimization (GWO), whale optimization algorithm (WOA) and moth flame optimization (MFO), in hybrid SVM-based models in this study. In addition, a 5-fold cross-validation resampling technique was used in the optimization stage of this paper to increase the reliability of the results. This shows that our paper is a different study and it can contribute in available literature in order to be used by other researchers, designers and engineers. Therefore, three SVM-based models, namely GWO-SVM, WOA-SVM, and MFO-SVM, are proposed in this research to predict TBM AR. Actually, the role of the GWO, MFO and WOA techniques is to optimize the hyperparameters 'C' and 'gamma' of the SVM model in order to get higher performance capacity for prediction purposes. This is an innovative work in the way that the idea of hybridization of SVM models is introduced and performed in forecasting TBM AR.

The rest of this paper is organized as follows:

After some descriptions regarding data and case study, the principle of the used AI and ML models and their modeling process will be explained. Then, the results of the SVM-based models in predicting TBM AR will be assessed and discussed in detail, and the best hybrid model among them will be selected and introduced in this field. Eventually, a sensitivity analysis on our data is conducted to identify the most important parameters on TBM AR.

2. Materials and methods

2.1. Dataset preparation

A total of 1286 data samples from the Pahang Selangor Raw Water Transfer (PSRWT) tunnel project in Malaysia were collected in this study to be used as a database to predict AR of TBM (Zhou et al., 2020a,e). This database was used in the construction of the SVM-based models, i.e., GWO-SVM, WOA-SVM, and MFO-SVM. Through the PSRWT tunnel, water is transferred from Pahang to Selangor in order to efficiently mitigate the water shortage problems that may appear in future. The excavation of the tunnel was done in order to cross the Main Range granite. The height of the mountain forming the Peninsular Malaysia backbone is as high as 100 to 1400 m. It was planned to apply TBMs to three sections of the path and to use the commonly-employed drilling and blasting techniques in four sections (Fig. 2).

A comprehensive review was done on existing literature for the aim of identifying the parameters that can have the highest impact on TBM performance. In this sense, three sets of parameters were determined, namely specifications of the machines used, the properties of rock mass, and the properties of rock material (Bruines, 1998). Benardos and Kaliampakos (2004) maintained that the parameters with the highest influence on performance of TBMs are RMR, RQD, rock mass weathering, and UCS. According to a number of scholars (such as Mogana et al., 1998; Mogana, 2007; Yagiz, 2008), the extent to which rock mass is weathered has a considerable effect on the TBM performance. Based on Sapigni et al.'s (2002) findings, RMR and UCS have a significant impact on the performance of TBMs. In addition, they suggested to use BTS as a model input in predictive models in order to forecast TBM performance. Alvarez Grima et al. (2000) found an inverse connection between UCS and TBM performance. According to Farrokh et al. (2012), the tunnel diameter, RQD, UCS, the rock type, revolution per minute (RPM), and normal force of disc-cutter have the highest impact upon TBM performance. On the other hand, Mahdevari et al. (2014) maintain that the highest effects on TBM performance come from factors such as UCS, intact rock brittleness, BTS, and thrust force.

According to the above discussion, seven model inputs that have the greatest effect on TBM performance, i.e., trust force per cutter (TFC), UCS, RPM, BTS, RQD, weathering zone (WZ), and RMR, were set to forecast TBM AR. The 1286 data samples consist of 560 data samples of fresh rock-mass, 553 data samples of slightly weathered rock-mass, and 173 data samples of moderately weathered rock-mass. In order to observe/measure the relevant parameters, about 13 km of the tunnel was divided into average 10 m panels. In each panel, the relevant machine factors (such as RPM, stroke speed, boring energy, TFC, cutter head, and cutter head torque) and rock mass characteristics (such as joint conditions, WZ, water condition, rock mass strength) were recorded/observed. Additionally, some rock blocks were gathered to conduct some required experiments in laboratory like UCS, the Schmidt hammer, BTS, p-wave velocity, density, and point load strength. The experiments were completed in accordance with the methods suggested by International Society for Rock Mechanics (ISRM, 2007).

The minimum, maximum, and average values of the model inputs and model output together with some other information are presented in Table 2. In Table 2, the ratings of the fresh, slightly and moderately WZs are considered as 1, 2 and 3, respectively. It should be noted that the similar procedure was implemented in the work accomplished by Benardos and Kaliampakos (2004). Full details of the collected/measured data of the PSRWT tunnel can be found in the work performed by Armaghani et al. (2019). The relationships between the input variables and the output from the matrix analysis chart, as well as two regression lines in each plot in the lower diagonal elements, are presented in Fig. 3. In addition, the violin plots which demonstrate the distribution of the TBM AR data with each input and output are displayed in Fig. 4. In the following sections, backgrounds of the AI models used in this study will be presented.

2.2. Support Vector Machine (SVM)

The SVM proposed by Vapnik (1995) is a supervised learning method that can be widely-used in statistical classification and regression analysis. The original model of SVM is to detect the best separation hyperplane in the feature space (FS) such that the negative and positive sample intervals on the training set are the largest. At the beginning, SVM was only applied for solving classification problems, and then, after introducing the ε-insensitive loss function (ε-ILF), it has been applied for implementing linear or non-linear regression tasks as indicated in Fig. 5(a, b). In this study, the SVM techniques will be applied as a regression analyzer. Therefore, this section will introduce and describe how to utilize the SVM technique to resolve regression problems. $(x_1, y_1), (x_2, y_2) \cdots (x_n, y_n)$ is a given training data set, $D_k = (x_k, y_k)$ represents the kth training sample, n is the number of training data, and the input space is represented by $x \in R^{\mathrm{M}}$ (here M represents M-dimensional). The purpose of the SVM regression is to make all sample points approach the hyperplane in order to minimize the total deviation between the sample points and the hyperplane (Gunn, 1998; Cherkassky and Ma, 2004; Shi et al., 2012; Li et al., 2020).

If these sample points have a linear relationship, the linear regression function can be described as follows:

$$f(x) = w \cdot x + e \tag{1}$$

As for nonlinear regression problems, each sample point is mapped to a high-dimensional FS with a nonlinear function $\phi(x)$. In this way, the nonlinear regression of the original space is transformed into a linear problem, and then the linear regression analyzer is performed in the high-dimensional FS. Therefore, the decision function of SVM regression can be presented in the following form (Gunn, 1998; Cherkassky and Ma, 2004; Li et al., 2020):

$$f(x) = w \cdot \varphi(x) + e(2) \tag{2}$$

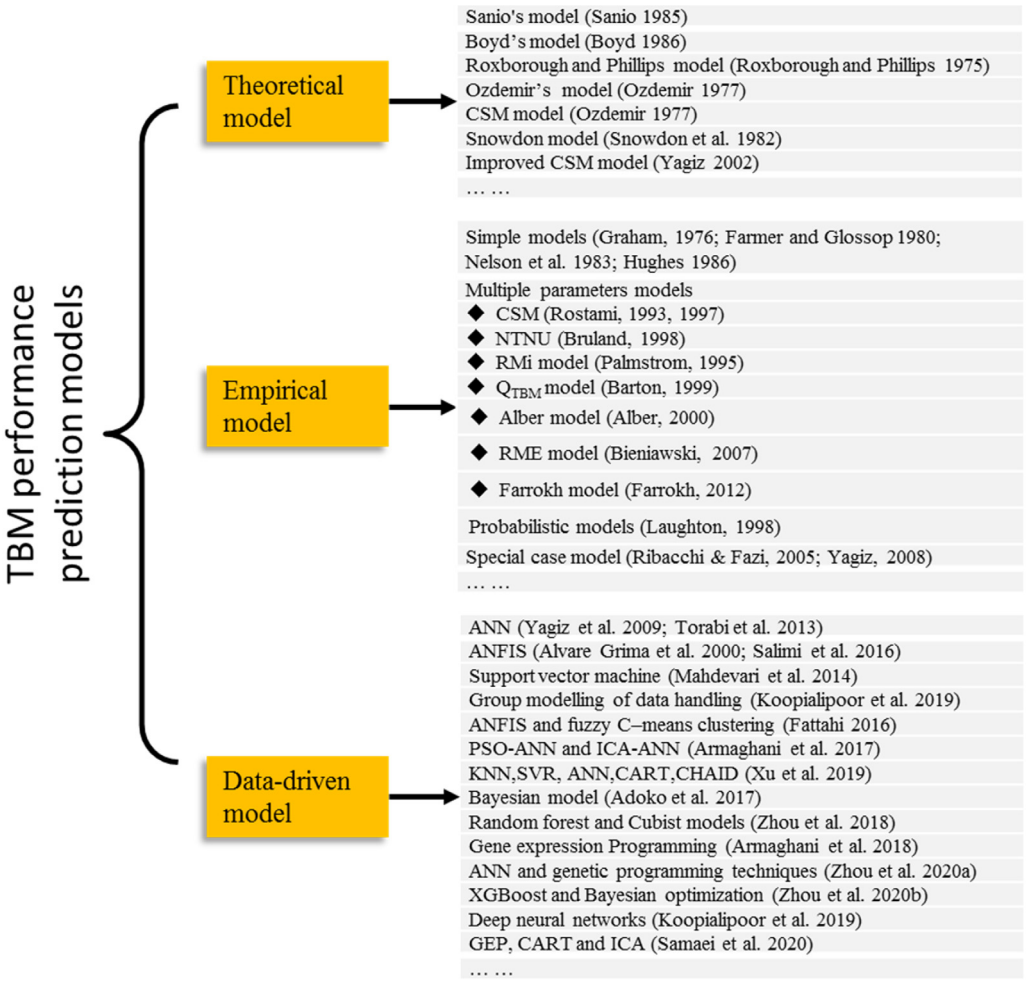

Fig. 1. The most cited applications of theoretical, empirical and data-driven approaches for TBM performance prediction.

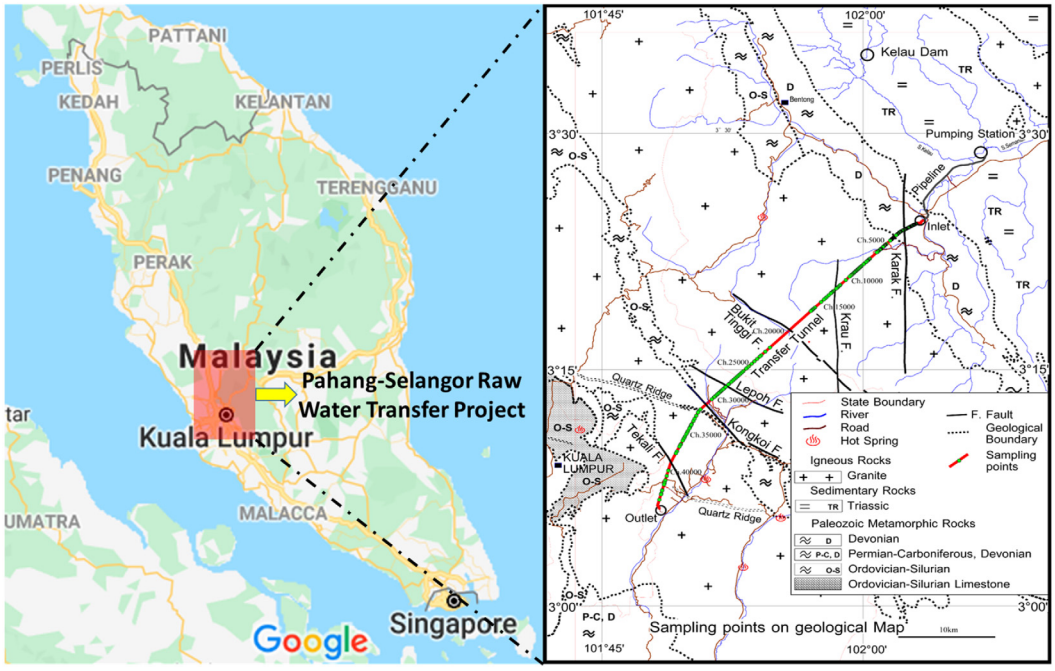

Fig. 2. The tunnel route view and its location of PSRWT tunnel in Malaysia.
Source: Resourced from Google Earth and (Zhou et al., 2020a).

Table 2
Summary of variables definition.

Parameter	Mean	S.d.	Median	Min.	Max.	Range	Skew	Kurtosis
RQD	54.259	28.610	51.625	6.250	95.000	88.750	−0.039	−1.525
UCS	135.128	45.104	152.100	40.000	194.000	154.000	−0.455	−1.301
RMR	72.894	16.101	76.500	44.000	95.000	51.000	−0.340	−1.350
BTS	10.321	4.066	8.990	4.690	15.680	10.990	−0.020	−1.774
WZ	1.699	0.693	2.000	1.000	3.000	2.000	0.479	−0.859
TFC	301.514	88.266	282.530	80.603	565.840	485.237	0.270	−0.145
RPM	8.827	2.314	9.331	4.040	11.950	7.910	−0.289	−1.467
AR	1.083	0.663	0.952	0.017	5.000	4.983	1.123	2.155

Note: BTS, Brazilian tensile strength, MPa; UCS, Uniaxial compressive strength, MPa; RMR, Rock mass rating; RQD, Rock quality designation/%; WZ, Weathering zone; TFC, Trust force per cutter, kN; RPM, Revolution per minute, rev per min; AR, Advance rate, meter per hour.

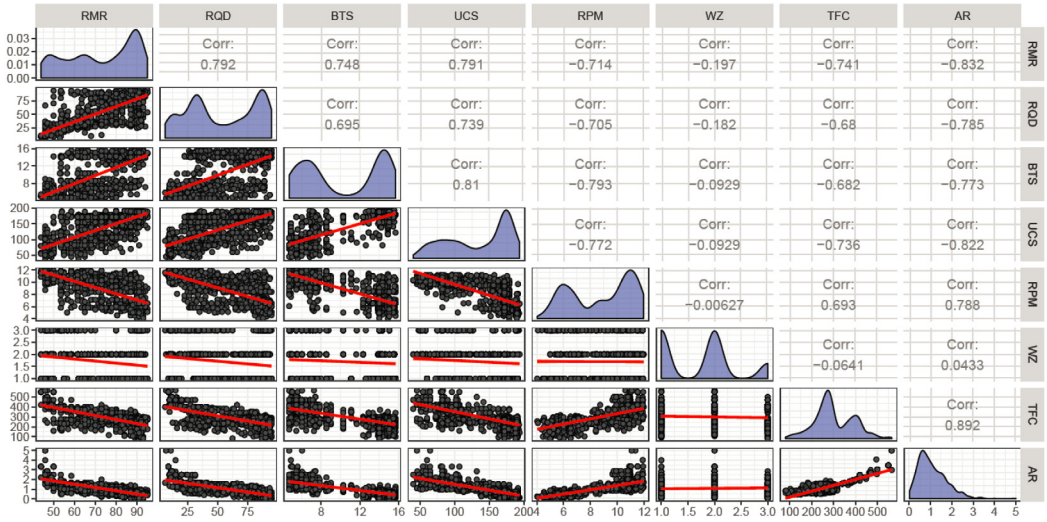

Fig. 3. Correlation scatterplot matrix of TBM AR dataset.

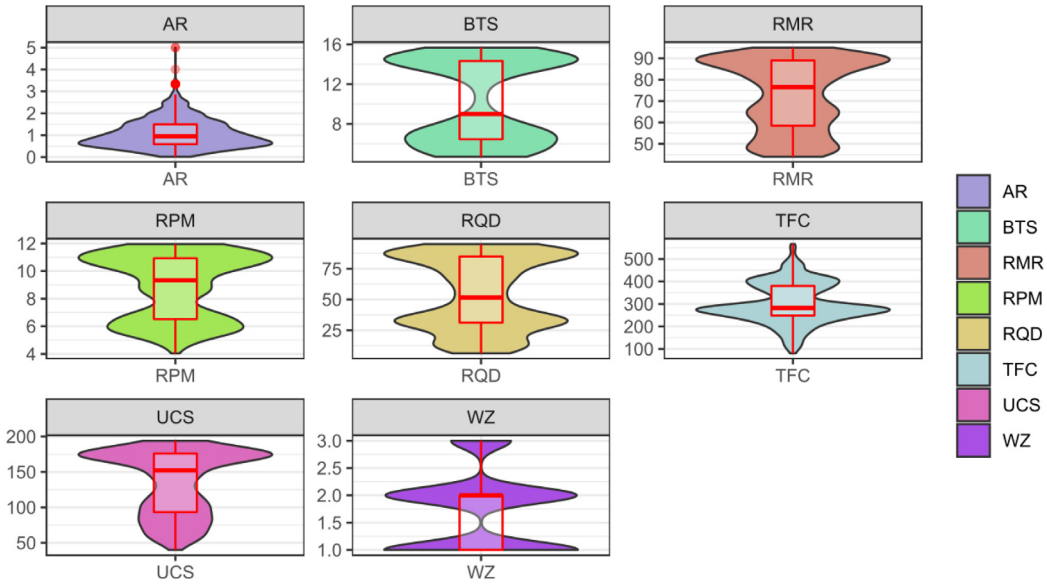

Fig. 4. Violin plots of TBM AR database used in SVM-based modeling process.

where w is the weight vector, e refers to model error values, and $\varphi(\mathrm{x})$ is a nonlinear function that can transform the nonlinear problem into a linear problem.

If there is a hyperplane $f(x) = w \cdot \varphi(x) + e$ in the space of R^M such that $|f(x) - y| \leq \varepsilon$ $(\varepsilon > 0)$, then $f(x) = w \cdot \varphi(x) + e$ is called ε-linear regression (Vapnik, 1995; Gunn, 1998; Cherkassky and Ma, 2004; Li et al., 2020). The ε- insensitive loss function is as follows:

$$\min \frac{1}{2} \|\mathbf{w}\|^2 \tag{3}$$

subject to

$$\left|\mathbf{w} \cdot \mathbf{x}_k + b - y_k\right| \leq \varepsilon, \qquad k = 1, 2, \ldots, n. \tag{4}$$

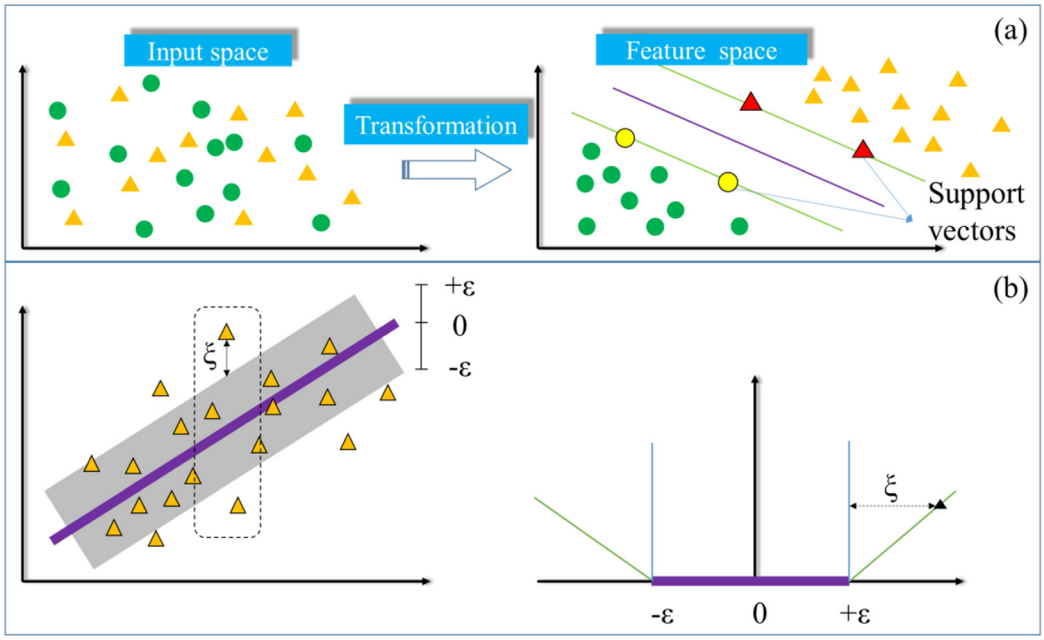

Fig. 5. (a) Data space transformation by SVM, and (b) Linear SVM regression using the ε –ILF.

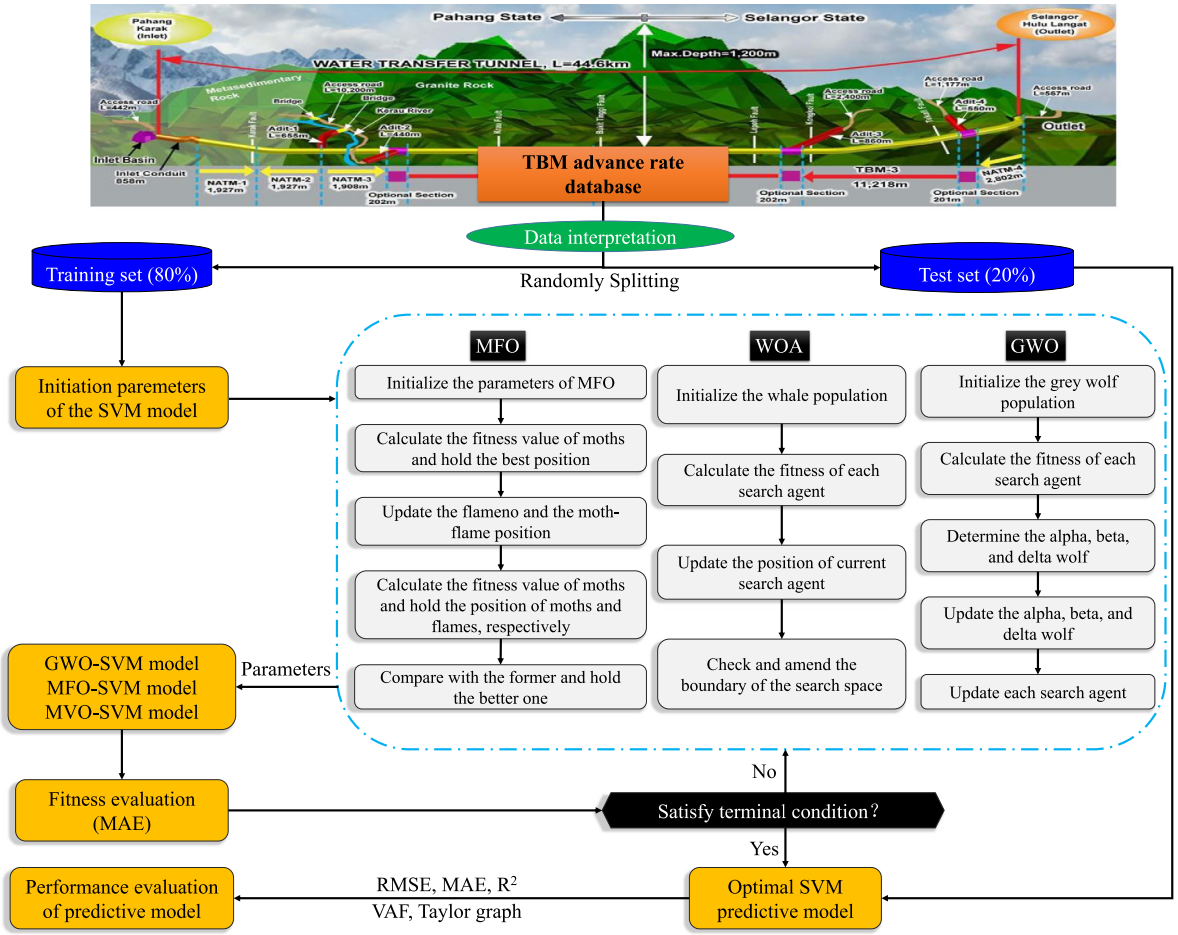

Fig. 6. Flowchart of hybrid intelligence models based on SVM optimized by GWO, WOA and MFO techniques.

In order to deal with inseparable data points and ensure that the constraint condition is feasible, introducing two slack variables, i.e., ξ, ξ^*, and the punishment coefficient, i.e., C (tuning the tradeoff between empirical deviations and the complication of the model), is of interest.

Then, Eqs. (3) and (4) are transformed into the following convex

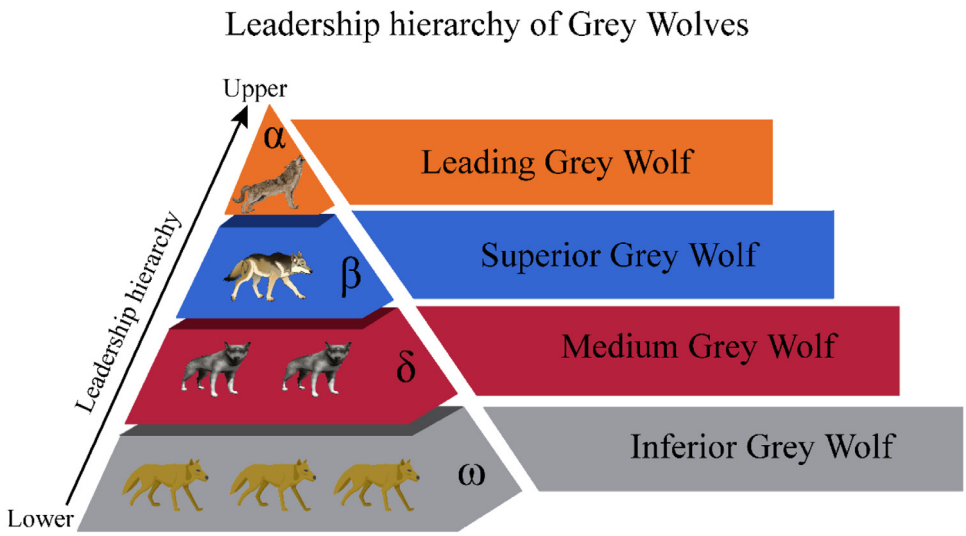

Fig. 7. Leadership hierarchy of gray wolves in nature.

optimization problem:

$$\min \frac{1}{2}\|\mathbf{w}\|^2 + C\sum_{k=1}^{n}(\xi_k + \xi_k^*) \tag{5}$$

$$\text{s.t.}\begin{cases}(\mathbf{w}\cdot\mathbf{x}_k + e) - y_k \le \varepsilon + \xi_k \\ y_i - (\mathbf{w}\cdot\mathbf{x}_k + e) \le \varepsilon + \xi_k^* \\ \xi_k \ge 0, \xi_k^* \ge 0 \\ k = 1, 2\ldots, n\end{cases} \tag{6}$$

Further, by introducing the Lagrange function, Eq. (7) can be optimized to a new form as shown in Eq. (9):

$$\min = \left\{ L = \frac{1}{2}\|\mathbf{w}\|^2 + C\sum_{k}^{n}(\xi_k + \xi_k^*) - \sum_{k=1}^{n}\alpha_k(\varepsilon + \xi_k - y_k + f(\mathbf{x_k})) - \sum_{k=1}^{n}\alpha_k^*(\varepsilon + \xi_k - y_k + f(\mathbf{x_k})) - \sum_{k=1}^{n}(\beta_k\xi_k + \beta_k^*\xi_k^*)\right\} \tag{7}$$

where $\alpha_k, \alpha_k^*, \beta_k, \beta_k^*$ are Lagrange multipliers. Eq. (9) can be transformed into the following function through dual transformation:

$$\min = \left\{ \frac{1}{2}\sum_{k,j=1}^{n}(\alpha_k^* - \alpha_k)(\alpha_j^* - \alpha_j)\mathbf{x}_k\mathbf{x}_j - \sum_{k=1}^{n}(\alpha_k^* - \alpha_k)y_k + \sum_{k=1}^{n}(\alpha_k^* + \alpha_k)\varepsilon \right\} \tag{8}$$

$$\text{s.t.} \quad \sum_{k=1}^{n}(\alpha_k - \alpha_k^*) = 0, \quad 0 \le \alpha_k, \alpha_k^* \le C. \tag{9}$$

The kernel function is able to map the input data to a high-dimensional FS [44]. In addition, these kernel functions can solve the problems with too many dimensions. There are commonly four main kernel functions of SVM, i.e., the linear, the radial basis function (RBF), the polynomial and the sigmoid (Gunn, 1998; Cherkassky and Ma, 2004; Pal and Deswal, 2008; Khandelwal, 2011; Shi et al., 2012; Zhou et al., 2012; Ceryan et al., 2013; Farfani et al., 2015; Li et al., 2020; Yu et al., 2020b; Zheng et al., 2020). Among them, the RBF of the Gaussian kernel function has been proved to have a good generalization ability for many kinds of datasets. Therefore, the authors of this article decided to use the RBF kernel. Further, introducing the kernel function satisfies the Mercer condition to replace the inner product of the linear regression condition. Finally, the nonlinear regression function can be described as (Gunn, 1998; Cherkassky and Ma, 2004; Li et al., 2020):

$$f(x) = \sum_{k=1}^{n}(\alpha_k^* - \alpha_k)K(\mathbf{x}_k, \mathbf{x}) + e \tag{10}$$

In the Gaussian kernel function of the SVM, the optimal parameters are considered as C (penalty factor) and g (RBF kernel deviation). In order to decrease the parametric searching time and conduct the parametric optimization process, several metaheuristic algorithms such as genetic algorithm, particle swarm optimization, gravitational search algorithm, ant lion optimizer, firefly algorithm, bat algorithm, league championship algorithm, symbiotic organisms search, imperialist competitive algorithm and charged system search algorithm (Abderazek et al., 2020; Champasak et al., 2020; Hamza et al., 2018; Karagöz and Yıldız, 2017; Karen et al., 2006; Kiani and Yildiz, 2015; Kurtuluş and Yıldız, 2020; Yildiz and Öztürk, 2010; Le et al., 2019; Yıldız, 2020b,c; Momeni et al., 2014, 2020; Yıldız and Yıldız, 2019; Nenavath et al., 2018; Zhou et al., 2012, 2019a,b, 2020c; Wang et al., 2018, 2020; Yu et al., 2020c; Zhang et al., 2020a) have been applied for determination of optimal hyper-parameters of the SVM model (Shi et al., 2012; Zhou et al., 2012; Li et al., 2020; Yu et al., 2020a) and other supervised machine learning models (Altan et al., 2019; Banan et al., 2020; Fan et al., 2020; Karasu et al., 2017, 2018; Karasu and Altan, 2019; Wu and Chau, 2013; Zhou et al., 2015, 2016, 2017a, 2019a,b,c, 2020f) To compare the performance of different optimal algorithms, three new metaheuristic techniques, i.e., GWO, WOA and MFO, were selected in this study to improve the prediction capability of the SVM in predicting TBM AR. Fig. 6 depicts a general implementation process of the SVM-based models optimized by GWO, WOA and MFO optimization scenarios. Additionally, Fig. 6 shows the optimization procedures applied by each optimization technique, i.e., GWO, WOA and MFO, and their roles in three hybrid models of WOA-SVM, GWO-SVM and MFO-SVM for predicting TBM AR.

2.3. Gray Wolf Optimization (GWO)

The GWO algorithm was proposed by Mirjalili et al. (2014) to solve optimization problems. This algorithm is an optimized search method inspired by the activity of the gray wolf predation. It can mimic the dominance hierarchy and hunting mechanism of the gray wolves in nature Yu et al., 2020b; Yildiz and Yildiz, 2018; Saxena et al., 2020. Due to its simple derivativefree and adaptable structure, the algorithm can be applied to experiments by searchers in different phases, i.e., initialization phase, bridging phase and position updating phase. GWO considers three best solutions as the leaders to update the positions of the other solutions. Its optimization process includes the steps of the gray wolf's social hierarchy, tracking, encircling and attacking prey. The specific steps are as follows:

(1) Gray wolf population initialization.

In this step, control parameters will be set, such as population size and stopping criterion. Subsequently, generating one initial population is performed randomly in the decision space (Liu et al., 2020b).

(2) Social hierarchy.

When designing GWO, we first need to build a hierarchical model of the gray wolf society. Calculating the fitness of each individual in the population, the three gray wolves with the best fitness among the wolves are marked by α, β, δ in sequence, and the remaining gray wolves are labeled by ω. That means there are four different groups in the wolf population which have a very strict social hierarchy similar to the pyramid (Yu et al., 2020b; Liu et al., 2020b), as shown in Fig. 7. The social rank in the gray wolf groups from high to low can be done through the use of α, β, δ, and ω, respectively. The optimization process of GWO is mainly guided by the best three solutions in each generation population (α, β, δ). The alpha heads the wolves to hunt prey, and the omegas receives the leadership of the three leaders.

(3) Encircling prey.

As one of the first steps of hunting, the gray wolf will gradually approach and encircle a prey. The encircling behavior can be expressed as a mathematical model in the following equations (Hu et al., 2020):

$$\begin{aligned} \boldsymbol{X}(t+1) &= \boldsymbol{X}_p(t) - \boldsymbol{A}\cdot\boldsymbol{D} = \boldsymbol{X}_p(t) - (2\mathbf{a}\gamma_1 - \mathbf{a})\cdot\left[\boldsymbol{C}\cdot\boldsymbol{X}_p(t) - \boldsymbol{X}(t)\right] \\ &= \boldsymbol{X}_p(t) - (2\mathbf{a}\gamma_1 - \mathbf{a})\cdot\left[2\gamma_2\cdot\boldsymbol{X}_p(t) - \boldsymbol{X}(t)\right] \end{aligned} \tag{11}$$

where t is the latest iteration, $\mathbf{X}_p(t)$ indicates the position vector of the prey, $X(t)$ presents the position vector of the current gray wolf, $X(t+1)$ is the position of the gray wolf in the next iteration, A and C are the coordination coefficient vectors, γ_1 and γ_2 are random numbers between [0, 1], and the **a** vector is linearly decreased from 2 to 0.

(4) Hunting the prey.

Hunting the prey includes three steps: firstly, recognizing the position of prey; secondly, encircling them; an finally, getting closer and harassing it. This process is usually conducted by the three leaders (i.e., α, β, δ). However, the solution space characteristics of many problems are unknown, and the gray wolf cannot determine the precise position of the prey (optimal solution). To simulate the hunting behavior of gray wolves, we assume that these three wolves have a strong ability to identify the location of potential prey (Yu et al., 2020b; Liu et al., 2020b). Therefore, the GWO always retains the best three gray wolves in the current population at each iteration and then updates the positions of other gray wolves based on their position information (Sexena et al. 2020). The equations for updating are presented as follows:

$$\begin{aligned} \boldsymbol{X}(t+1) &= \left(\boldsymbol{X}_1 + \boldsymbol{X}_2 + \boldsymbol{X}_3\right)/3 \\ &= \left[\left(\boldsymbol{X}_\alpha - \boldsymbol{A}_1\boldsymbol{D}_\alpha\right) + \left(\boldsymbol{X}_\beta - \boldsymbol{A}_2\boldsymbol{D}_\beta\right) + \left(\boldsymbol{X}_\delta - \boldsymbol{A}_3\boldsymbol{D}_\delta\right)\right]/3 \\ &= \left[\left(\boldsymbol{X}_\alpha - \boldsymbol{A}_1(\boldsymbol{C}_1\boldsymbol{X}_\alpha - \boldsymbol{X})\right) + \left(\boldsymbol{X}_\beta - \boldsymbol{A}_2(\boldsymbol{C}_2\boldsymbol{X}_\beta - \boldsymbol{X})\right)\right. \\ &\quad \left. + \left(\boldsymbol{X}_\delta - \boldsymbol{A}_3(\boldsymbol{C}_3\boldsymbol{X}_\delta - \boldsymbol{X})\right)\right]/3 \end{aligned} \tag{12}$$

The equations represent the position updating according to alpha, where $\boldsymbol{X}_1$, $\boldsymbol{X}_2$ and $\boldsymbol{X}_3$ are the positions of the α, β, δ wolves, respectively, and $\boldsymbol{D}_\alpha$, $\boldsymbol{D}_\beta$, and $\boldsymbol{D}_\delta$ are the distances of the prey from the α, β, δ wolves, respectively.

2.4. Whale Optimization Algorithm (WOA)

WOA is one of the swarm-based algorithms inspired by the hunting of prey of the humpback whale (Mirjalili and Lewis, 2016). It uses a unique technique based on the special bubble-net and the feeding behavior of the whale. To hunt the prey, the whale performs three steps: (i) encircling prey; (ii) exploitation (bubble-net attacking); and (iii) exploration (searching for prey). The details of the WOA can be found in the following investigations (Mirjalili and Lewis, 2016; Mafarja and Mirjalili, 2017; Guo et al., 2019). In this study, the WOA is used to optimize the capacity of the SVM in predicting TBM AR (i.e., WOA-SVM).

i. Encircling prey

Each humpback whale represents an individual, and the position of each individual in the search space represents a solution. The whale can identify the location of the prey and encircle the prey through echolocation. The update formula of the whale location is as follows:

$$\mathbf{X}^{t+1} = \mathbf{X}^t_{gbest} - A\cdot\left|C\cdot\mathbf{X}^t_{gbest} - \mathbf{X}^{\mathbf{t}}\right| \tag{13}$$

where t represents the current iteration, $\mathbf{X}^{\mathrm{t}}$ is the current position vector, the position vector of the best solution obtained so far is indicated by $\mathbf{X}^t_{gbest} = (\mathbf{X}^t_{gbest1}, \mathbf{X}^t_{gbest2}, \ldots \mathbf{X}^t_{gbestD})$, D is vector dimension, $A\cdot\left|C\cdot\mathbf{X}^t_{gbest} - \mathbf{X}^{\mathbf{t}}\right|$ is encircling step-size, and the coefficient vectors (A and C) are defined as follows:

$$A = 2a\cdot rand_1 - a \tag{14}$$

$$C = 2\cdot rand_2 \tag{15}$$

where, $rand_1$&$rand_2$ are random numbers generated by a uniform distribution in $[0, 1]$, a is linearly decreased from 2 to 0 over the course of iterations, and it can be represented by the following equation:

$$a = 2 - 2t/t_{\max} \tag{16}$$

ii. Bubble-net attacking

It can be seen from Fig. 8 that the whale attacks the prey by spiraling up and continuously shrinking the encircling. Two methods (shrinking encircling mechanism & spiral updating position) are designed to describe the bubble-net behavior mathematically, and their explanations are presented as follows:

The shrinking encircling mechanism is achieved by decreasing the value of a in Eq. (14). At the same time, the fluctuation range of the coefficient vector A also decreases with a. When a decreases from 2 to 0 in the iterative process, the fluctuation range of A is $[-a, a]$. When A represents the random number in $[-1,1]$, the new position ($\mathbf{X}^{t+1}$) can be defined anywhere between the current position ($\mathbf{X}^{\mathbf{t}}$) and the current position of the best solution obtained so far ($\mathbf{X}^t_{gbest}$). It means that the whale always swims in the contracting circle.

In spiral updating position, the humpback whale swims to the prey in a spiral mode of motion, and the mathematical model is as follows:

$$\mathbf{X}^{\mathbf{t+1}} = \mathbf{X}^t_{gbest} + D\cdot e^{bl}\cdot\cos(2\pi l) \tag{17}$$

where, $D = |X^t_{gbest} - \mathbf{X}_t|$ is the distance between the whale and the prey (best solution obtained up to now), b is a constant for restricting the shape of the logarithmic spiral, and l is a random number in $[-1,1]$ (Mirjalili and Lewis, 2016).

Humpback whales swim around the prey within a shrinking circle and along a spiral-shaped path simultaneously. In order to simulate this simultaneous behavior, it is assumed that there is a probability of 50% to the choose shrinking encircling mechanism or spiral updating position to update the position of whales (Mirjalili and Lewis, 2016). The mathematical formula is presented as follows:

$$\mathbf{X}^{t+1} = \begin{cases} \mathbf{X}^t_{gbest} - A\cdot\left|C\cdot\mathbf{X}^t_{gbest} - \mathbf{X}^t\right|, p < 0.5 \\ \mathbf{X}^t_{gbest} + D\cdot e^{bl}\cdot\cos(2\pi l), p \geq 0.5 \end{cases} \tag{18}$$

where p is a random number in the range of [0,1].

iii. Search for prey

When the coefficient vector $|A| > 1$, it means that the whale swims outside the shrinking encircling circle. At this time, the humpback whale searches randomly according to each other's positions. The mathematical model is described as follows:

$$\mathbf{X}^{t+1} = \mathbf{X}^t_{rand} - A\cdot\left|C\cdot\mathbf{X}^t_{rand} - \mathbf{X}^t\right| \tag{19}$$

where $\mathbf{X}^t_{\mathrm{rand}}$ is a position vector of a whale individual randomly chosen from the current population.

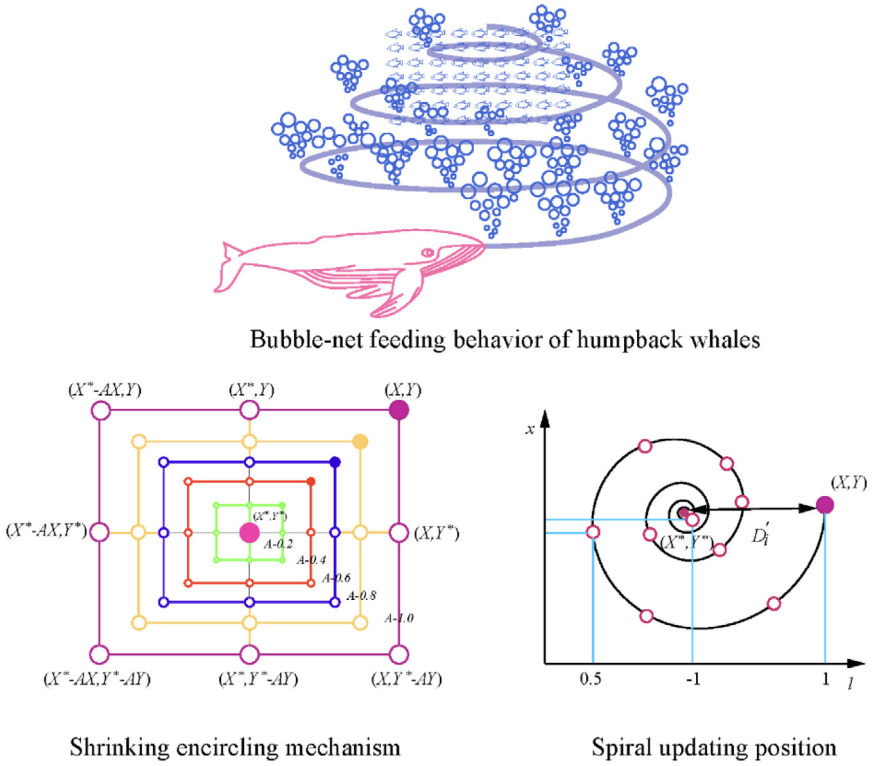

Fig. 8. Strategy and bubble-net search mechanism of the WOA (Mirjalili and Lewis, 2016).

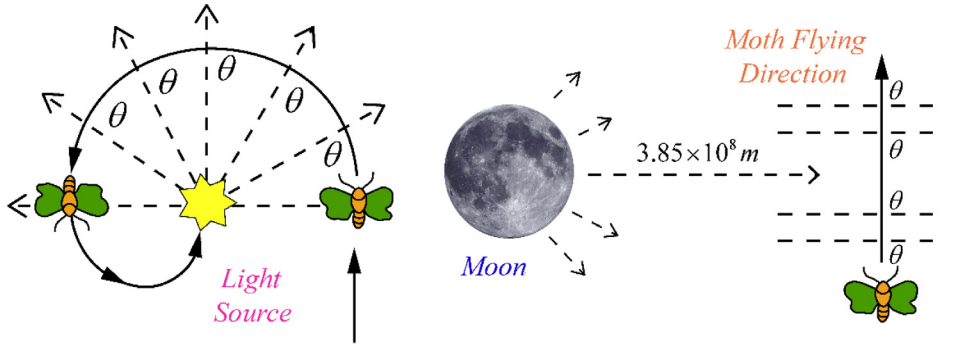

Fig. 9. Orientation behavior of moth swarm.

2.5. Moth-Flame Optimization (MFO)

The MFO algorithm is a group intelligent optimization inspired by the transverse orientation–navigation behavior of moths (Mirjalili, 2015). In this flying behavior, a moth flies by maintaining a fixed angle with respect to the moon, a very effective mechanism for traveling long distances in a straight path (Mirjalili, 2015; Yıldız, 2020a). The conceptual model of transverse orientation is shown in Fig. 9(a). However, it is only helpful for moving in straight line when the light source is very far. When moths see an artificial light, they try to maintain a similar angle with the light to fly in straight line. However, because artificial light is pretty close to the moon, using the same navigation method will produce useless or deadly spiral flight paths, and moths will eventually converge into light (Mirjalili, 2015). A conceptual model of this behavior can be demonstrated in Fig. 9(b). The MFO algorithm consists of several steps, which are presented below, The framework of the MFO algorithm can be briefly presented as follows:

$$MFO = (I, P, T) \tag{20}$$

$$I: \phi \rightarrow \{M, OM\} \tag{21}$$

$$P: M \rightarrow M \tag{22}$$

$$T: M \rightarrow \{true, false\} \tag{23}$$

where I is the function that produces a random population of moths and corresponding fitness values; P is the main function that moves the moths around the search space; T is the function that returns true or false whether the stopping criterion is satisfied or not; and M is the position matrix of moths.

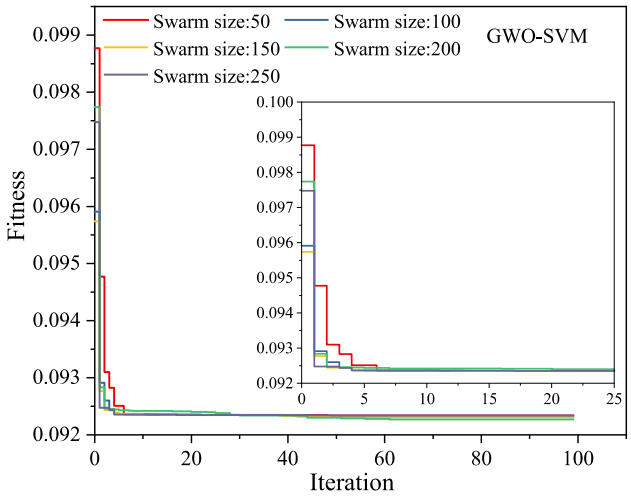

(a) GWO-SVM

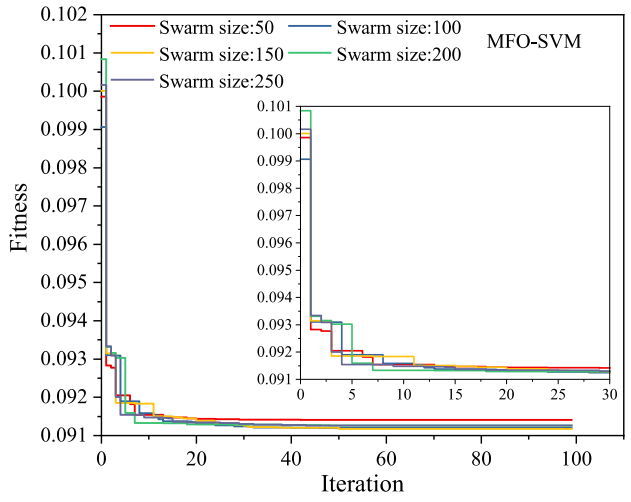

(b) MFO-SVM

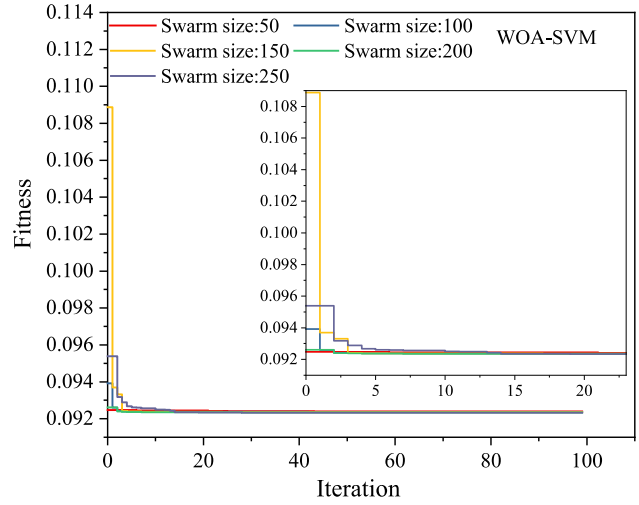

(c) WOA-SVM

Fig. 10. Optimization models for different swarm sizes.

After the initialization, the P function is iteratively run until the T function returns true. The P function is the main function that moves the moths around the search space.

In order to mathematically model the transverse orientation behavior of moth flight, the MFO algorithm uses a logarithmic spiral as the main update mechanism of moths, and the position of each moth with respect to a flame will be updated by using Eq. (24).

The following equation is applied in the MFO algorithm to update the position of moths in each iteration.

$$M_i = S(M_i, F_j) = D_i \cdot e^{bt} \cdot \cos(2\pi t) + F_j \tag{24}$$

where M_i and M_j represent the ith moth and the jth flame, respectively; S is the spiral function, D_i indicates the distance between M_i and M_j, b is a constant ($b = 1$), and t is a random number with the range of [−1,1].

To improve the exploration of optimal strategy, Eq. (25) is employed to decrease the number of flames during iteration.

$$flame - no = round(N - l * \frac{N-1}{T}) \tag{25}$$

where N is the maximum number of flames, l and T are the current number of the iteration and the maximum number of iterations, respectively.

2.6. SVM-based model verification and evaluation

After building the aforementioned models, it is necessary to understand whether the model used has evolved sufficiently accurate results for the target used, and whether the quality of the test model is quite enough.

In this work, the training set is applied to train the prediction models, and the test set is used to verify the prediction models. Moreover, the relevant evaluation indicators— the coefficient of determination (R^2), the root mean squared error (RMSE), the mean absolute error (MAE), and the variance accounted for (VAF) — are applied to effectively evaluate the reliability of the hybrid models and interpret the relationship between the actual value and the predicted value. Note that the RMSE represents the standard deviation of the fitting error between the actual value and the predicted value. The value of R^2 represents the percentage of the square of the correlation between the predicted and actual values of the target variable. The mean absolute error is the average value of the absolute error, which can well reflect the actual situation of the predicted value error. The calculation formulas of the evaluation indicators are as follows (Altan and Hacıoğlu, 2020; Armaghani et al., 2014; Armaghani and Momeni, 2015; Bui et al., 2020; Bunawan et al., 2018; Ding et al., 2020; Faizollahzadeh Ardabili et al., 2018; Grima et al., 2000; Khandelwal and Singh, 2009; Li et al., 2020; Marto and Hajihassani, 2014; Rezaei et al., 2016; Shamshirband et al., 2019; Yildiz, 2013, 2017, 2019; Yildiz et al., 2020a; Yildiz and Yildiz, 2017, 2018; Yıldız, 2020a; Yildiz et al., 2020a; Yıldız et al., 2020b,c; Yıldız and Yıldız, 2019; Yong et al., 2020; Yu et al., 2020b; Zhang et al., 2020a,b,c; Zhou et al., 2017a,b, 2019a,b,d,e, 2020a,b,d,f):

$$RMSE = \sqrt{\frac{1}{N}\sum_{i=1}^{N}\left(A\hat{R}_i - AR_i\right)^2} \tag{26}$$

$$R^2 = 1 - \frac{\sum_{i=1}^{N}\left(AR_i - A\hat{R}_i\right)^2}{\sum_{i=1}^{N}\left(AR_i - A\overline{R}_i\right)^2} \tag{27}$$

$$MAE = \frac{1}{N}\sum_{i=1}^{N}\left|A\hat{R}_i - AR_i\right| \tag{28}$$

$$VAF = \left[1 - \frac{var\left(AR_i - A\hat{R}_i\right)}{var\left(AR_i\right)}\right] \times 100 \tag{29}$$

where AR_i represents the observed value, $A\hat{R}_i$ is the predicted value of the model, $A\overline{R}_i$ indicates the average of the observed values, and N denotes the number of samples in the training or testing stages.

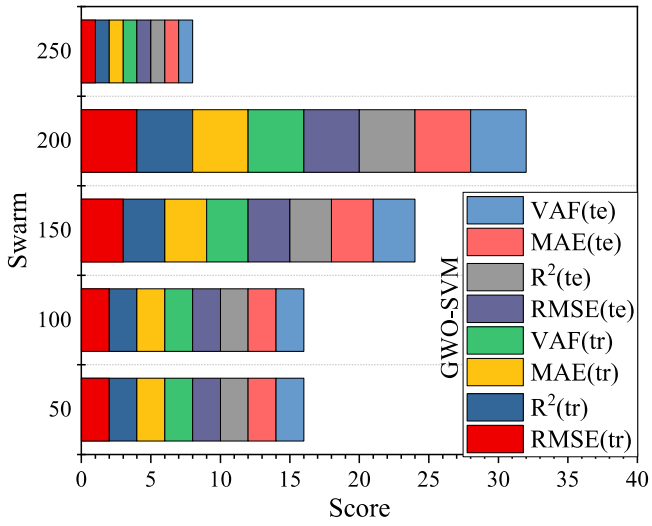

Fig. 11. Comprehensive sorted stacked graph for GWO-SVM with different cluster sizes.

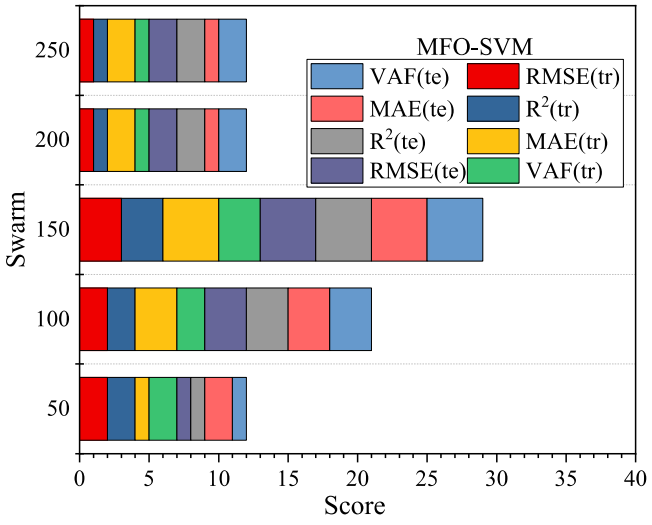

Fig. 12. Comprehensive sorted stacked graph for MFO-SVM with different cluster sizes.

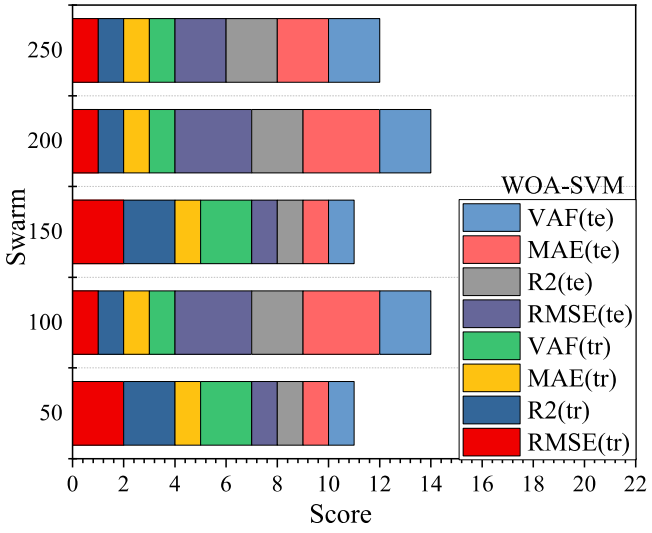

Fig. 13. Comprehensive sorted stacked graph for WOA-SVM with different cluster sizes.

3. SVM-based optimization techniques

In this study, the GWO, MFO, and WOA are applied to hyperparameter optimization of the prediction model based on SVM. After constructing many models, it is found that in each optimization process, the model calculation time will increase when the population sizes are too large as the number of iterations increases, and too small population sizes will produce unstable fitness values. Therefore, several groups of 50, 100, 150, 200, and 250 population sizes in the optimization model were selected for constructing models in this paper, and their iteration curves were drawn according to the corresponding fitness values. The results of fitness values together with their iteration numbers for GWO-SVM, MFO-SVM, WOA-SVM models in predicting TBM AR are shown in Fig. 10.

For the hybrid model based on SVM, the purpose of using the GWO, MFO, and WOA methods is to optimize the hyperparameters 'C' and 'gamma' of the SVM model. The ranges of these parameters are set to (0.01, 100) and (0.01, 50), respectively. The main process of optimizing SVM parameters using GWO, MFO, and WOA optimization techniques is as follows:

(1) Data preparation: The data set is randomly divided into a training set and a testing set according to an appropriate ratio.

(2) Initialization parameters: Set GWO, MFO, and WOA parameters, and the parameter settings of the three optimization algorithms are shown in Table 3.

(3) Fitness evaluation: Calculate the fitness function and evaluate its fitness before optimizing the target parameter value.

(4) Update parameters: According to the results of each iteration, adjust the optimization requirements that the hyperparameters meet.

(5) Stop condition checking: When the optimization stop requirement is reached, the best parameters are obtained.

Results of different swarm sizes used in GWO-SVM, MFO-SVM, WOA-SVM models based on R^2, RMSE, MAE, and VAF for training and test stages are tabulated in Figs. 10–13, respectively. Furthermore, rank values assigned to training and testing datasets together with their total rank values are shown in these tables.

4. Results and discussion

To explore better prediction methods for predicting TBM AR in this paper, three optimization algorithms (i.e., GWO, MFO, and WOA) were combined with SVM, and then these three SVM-based hybrid intelligent models were constructed using the training set. In the above optimization process, different hyperparameter configurations and different model prediction performances were obtained.

Table 3
Parameter size setting of the heuristic algorithm.

Algorithm	Parameters	Value
GWO (Gray wolf optimization)	Convergence constant a	Linear decrease [2,0]
MFO (Multi verse optimization)	*b* *l*	1 [−1,1]
WOA (Whale optimization algorithm)	*r* *a*	[0,1] Linear decrease [2,0]

Table 4
Comparison of the performance of SVM-based hybrid models with the same population size.

Model	Training								Score
	RMSE	Score	R^2	Score	MAE	Score	VAF (%)	Score	
GWO-SVM (Swarm:200)	0.1288	2	0.9612	2	0.0866	2	96.13	2	8
MFO-SVM (Swarm:150)	0.1269	3	0.9623	3	0.0835	3	96.24	3	12
WOA-SVM (Swarm:100/200)	0.13	1	0.9605	1	0.0876	1	96.06	1	4
Model	Testing								Score
	RMSE	Score	R^2	Score	MAE	Score	VAF (%)	Score	
GWO-SVM (Swarm:200)	0.1187	2	0.9709	2	0.0920	2	97.16	2	8
MFO-SVM (Swarm:150)	0.1155	3	0.9724	3	0.0894	3	97.34	3	12
WOA-SVM (Swarm:100/200)	0.1199	1	0.9703	1	0.0935	1	97.10	1	4

As shown in Fig. 10, the relationship between the number of different populations and the fitness value in each intelligent optimization is shown under the same number of iterations for GWO-SVM, MFO-SVM, WOA-SVM, respectively. Moreover, in Figs. 11, 12, and 13, a comprehensive prediction result of different populations for each hybrid model can be seen, intuitively (Zorlu et al., 2008). The comprehensive prediction score shows that the best population size of GWO-SVM is 200 and its prediction performance is (RMSE = 0.1187, R^2 = 0.9709, MAE = 0.0920, and VAF = 97.16); the best population size of MFO-SVM is 150 and its prediction performance is (RMSE = 0.1155, R^2 = 0.9724, MAE = 0.0894, and VAF = 97.34); and the best population size of WOA-SVM is 100 (or 200) and its prediction performance is (RMSE = 0.1199, R^2 = 0.9703, MAE = 0.0935, and VAF = 97.10).

The correlation between the predicted value and the actual value of TBM AR can be seen in Fig. 14. Also, Fig. 14 shows another type of performance prediction presentation for the SVM-based techniques. The results show that the training and test results of these intelligent models are excellent, and the training/test sample points are basically distributed near the perfect fitting line ("actual AR = predicted AR"). From the perspective of R^2, RMSE, MAE, and VAF, it can be seen that the prediction performance of the MFO-SVM hybrid model is slightly better than the two other SVM-based models. The R^2 value of its training set is 0.9623, the RMSE value is 0.1269, the MAE value is 0.0835, and the VAF value is 96.24; the R^2 value of its test set is 0.9724, the RMSE value is 0.1155, the MAE value is 0.0894, and the VAF value is 97.34. It should be mentioned that the MFO-SVM model is the better model among all three models for both training and test sections. Needless to say, these hybrid SVM models can significantly increase the performance capacity of a pre-developed SVM model in estimating TBM AR, as shown in Fig. 15. For instance, the RMSE value can be reduced from about 0.15 to 0.12 by developing SVM-based models.

Next, Table 4 summarizes the performance index results (RMSE, R^2, MAE, and VAF) and comprehensive ranking results of the three hybrid models (GWO-SVM, MFO-SVM, and WOA-SVM) in predicting TBM AR under the conditions of their respective optimal population sizes. It can be clearly seen that the result of combining the training set and the testing set is that the overall score of MFO-SVM is better. This shows that the MFO-SVM hybrid model has better accuracy and robustness in predicting TBM AR compared to the other two hybrid models.

To further analyze and compare the prediction performance of the aforementioned hybrid models, as shown in the Taylor graph (Fig. 16), models such as Random Forest Regression, Decision Tree, AdaBoost, and ANN were also added for comparison purposes.

The Taylor graph is more intuitive compared with a single graph of R^2 and RMSE. The Taylor graph can comprehensively display the standard deviation of multiple variables, the correlation coefficient with the reference value, and the root mean squared deviation on a two-dimensional graph, which can fully and clearly account for the simulation capabilities of multiple models. The Taylor graph results show that the prediction performance of the hybrid optimization models is more accurate than the other models, and among all models, the MFO-SVM model is slightly better. Based on the above results, it can be found that the MFO-SVM hybrid model has good learning, good evaluation, and prediction capabilities. Therefore, this article recommends using the proposed MFO-SVM hybrid model to predict TBM AR.

It is worth mentioning that the full data presented in this study were used in the study conducted by Armaghani et al. (2019). They used one more input parameter, i.e., quartz content, together with the seven inputs used in this study and developed two hybrid models of PSO–ANN and ICA-ANN for forecasting the TBM AR values. The R^2 results of these two hybrid models were obtained as (0.958 and 0.961) and (0.948 and 0.951) for training and testing phases of PSO–ANN and ICA-ANN models, respectively. The results of research conducted by Armaghani et al. (2019) and the present study showed that the MFO-SVM model developed in this study, with R^2 of (0.9623 and 0.9724 for training and test phases, respectively), is better than the PSO–ANN model of Armaghani et al. (2019), especially regarding testing data samples. In addition, Zhou et al. (2019b) used this data with six input parameters including RQD, UCS, RMR, TFC, RPM and BTS (without WZ) and proposed ANN and genetic programming (GP) models to predict TBM AR values. They obtained R^2 values of (0.897 and 0.916) and (0.854 and 0.875) for training and test phases of the GP and ANN predictive models, respectively, which confirmed that the MFO-SVM model proposed in this study is able to provide higher performance prediction capacity.

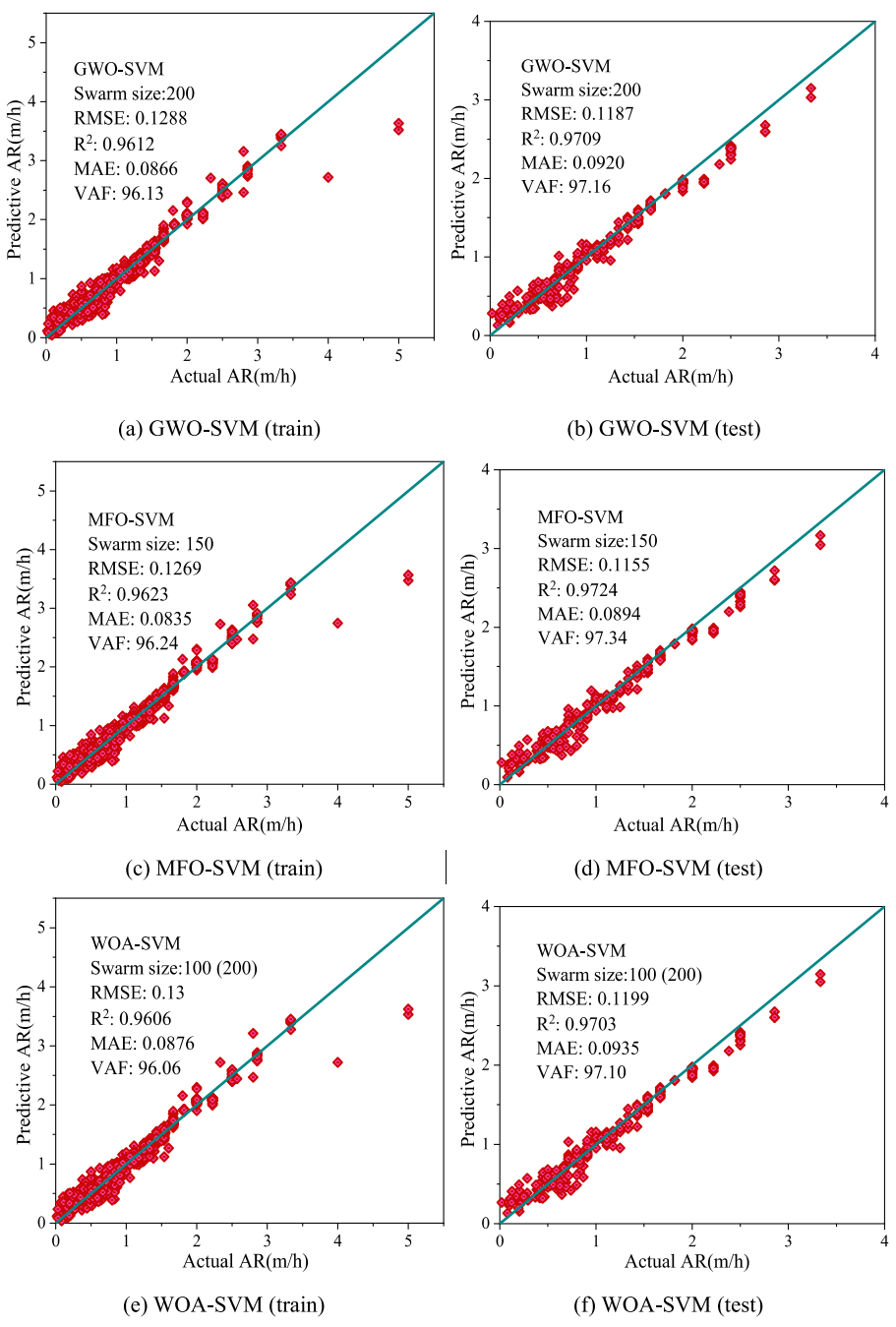

Fig. 14. Correlation and error analysis between TBM AR predicted value and the actual value obtained by three SVM-based models.

Aside from TBM AR, the results of this study are better than many published investigations in other TBM performance parameters such as PR. For example, R^2 values of 0.90, 0.67, 0.89 and 0.94 were obtained in the studies conducted by Yagiz et al. (2009), Yagiz and Karahan (2011), Ghasemi et al. (2014), and Koopialipoor et al. (2019), respectively, to predict PR of TBM introducing ANN, PSO, fuzzy logic and GMDH techniques. As a result, the developed MFO-SVM predictive model received a higher accuracy level compared to said models. Therefore, this article recommends applying and developing the MFO-SVM model for prediction of TBM AR.

5. Sensitivity analysis

Under certain rock conditions, the prediction of TBM AR is the key to mechanical tunnel engineering. To accurately predict the AR of TBM and reduce the high cost and risk of tunnel construction, various factors affecting AR must be comprehensively considered. It can be known that all input variables, i.e., RMR, RQD, BTS, UCS, WZ, TFC, and RPM, contribute to the prediction of TBM AR. However, the sensitivity of each input parameter is unclear and needs further study.

To explore and compare the sensitivity of different influencing factors to TBM AR, in this section, the mutual information test method (Verron et al., 2008) was used to analyze the importance of the input variables on TBM AR. Mutual information (MI) is a filtering method that can be used to capture the arbitrary relationship (including linear and nonlinear) between each feature and the label. It is a measure of the interdependence between variables and indicates the strength of the relationship between variables. The size of the MI between variables

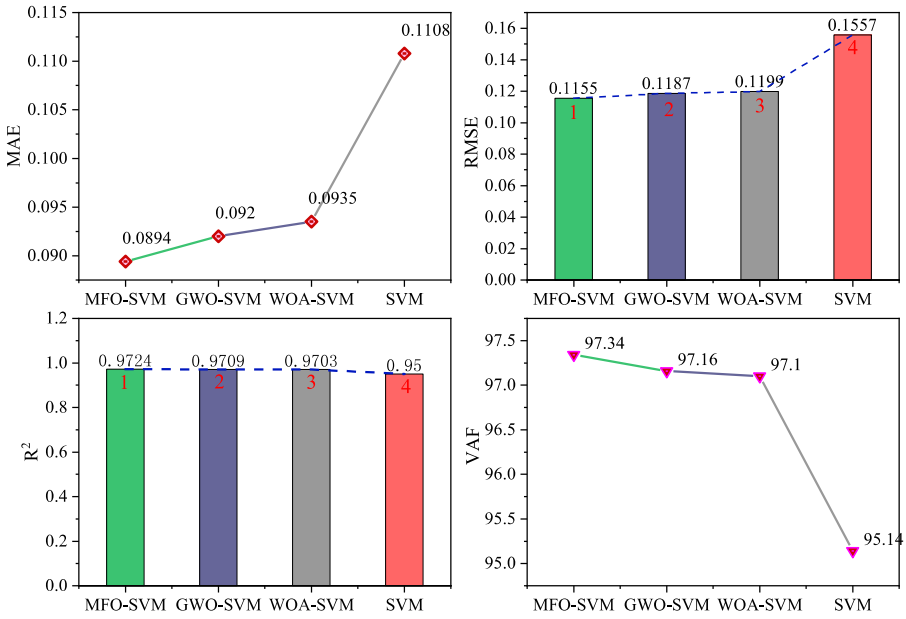

Fig. 15. Matrix diagram of model evaluation index.

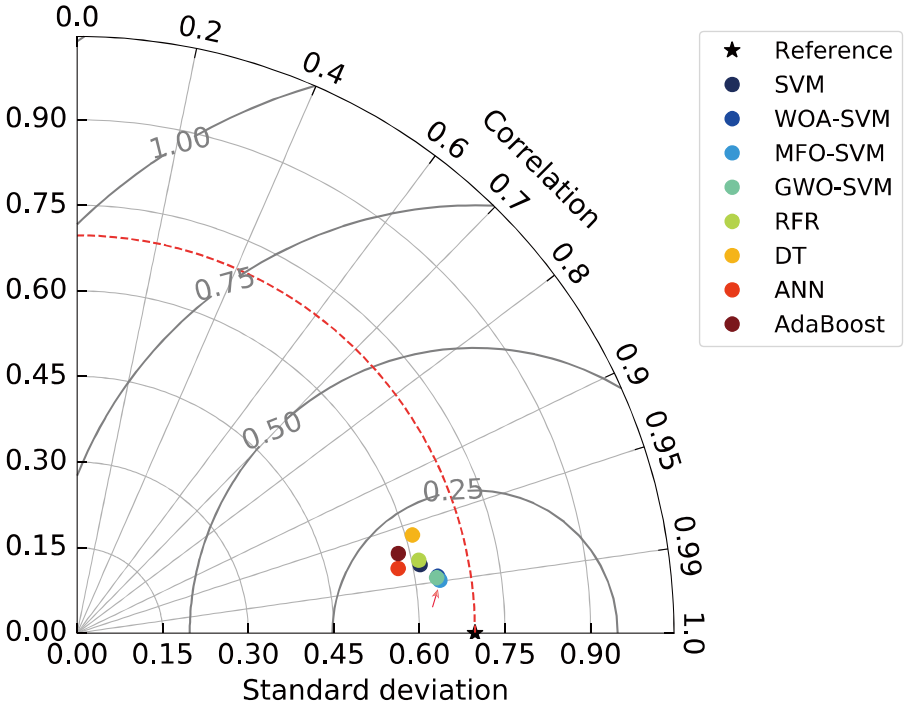

Fig. 16. Comparison of the performance of multiple models in Taylor graphs.

can be calculated by the information gain:

$$Gain(Y,X) = Ent(Y) - \sum_{v=1}^{V} \frac{|Y^v|}{|Y|} Ent(Y^v) \tag{30}$$

where, v represents the number of all possible values of X, Y^v represents the set of Y when x takes the value x_v, and $Ent(Y)$ represents the information entropy. The larger the value of $Gain(Y, X)$, the higher the correlation between X and Y.

Finally, according to the variable score in the mutual information test, the importance level of the input variable that predicts AR was determined. As shown in Fig. 17, from the analysis results, it can be clearly seen that TFC, RPM, and RMR are the most important variables for predicting TBM AR. Their importance scores respectively were obtained as 1.4513, 1.2889, and 1.0402. However, it should be noted that other model inputs, i.e., BTS, RQD, and UCS, have a deep impact on TBM AR. Therefore, when predicting TBM AR, TFC, RPM, RMR, UCS, RQD, and BTS are considered as the most important factors. As a result, WZ with a score of 0.0572 is not considered as an influential factor on TBM AR. It is important to mention that there is a need to consider more input variables as well as the number of samples to enrich the dataset in the future, so that the model can achieve better prediction accuracy and generalization.

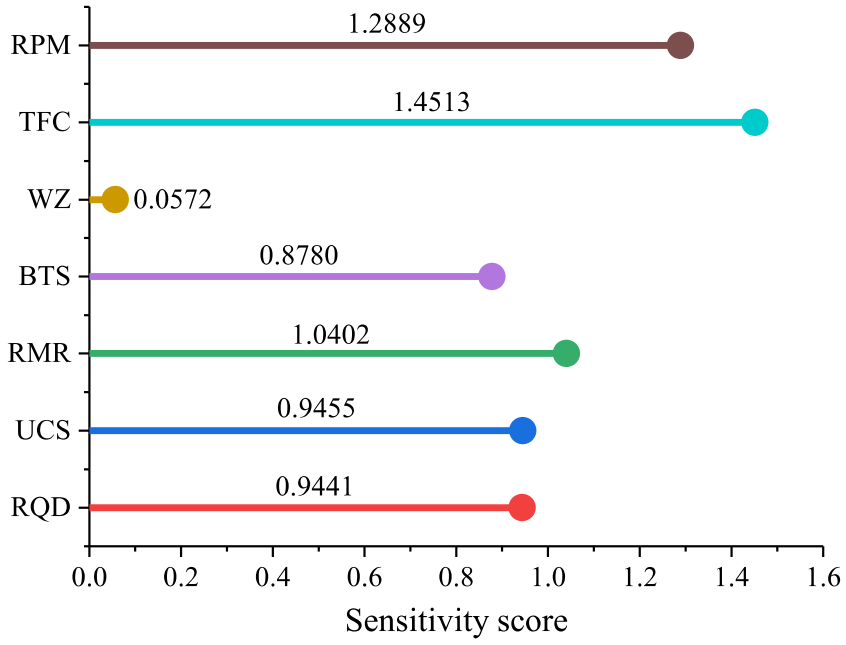

Fig. 17. Sensitivity analysis of seven indicators on TBM AR.

6. Conclusions

In this study, the idea of the hybridization of SVM models was applied in the field of TBM performance. To do that, three well-known optimization techniques i.e., GWO, MFO, and WOA which have been successfully examined by other researchers were selected and combined with SVM, and then GWO-SVM, MFO-SVM, WOA-SVM hybrid models were created for prediction purposes. These models were constructed using seven model inputs and an output which was TBM AR. The most influential factors of the GWO, MFO, and WOA were investigated, and according to them, we received the highest performance prediction of these hybrid models. The performance of the SVM-based models was assessed using RMSE, R^2, MAE, and VAF. Besides, for comparison purposes, we have predicted TBM AR proposing other models, i.e., SVM, Random Forest, ANN, AdaBoost, and Decision Tree. Eventually, after assessing the performance of all applied and constructed models, it was found that the MFO-SVM model with R^2 of (0.9623 and 0.9724), RMSE of (0.1269 and 0.1155), MAE of (0.0835 and 0.0894), and VAF of (96.24 and 97.34), respectively, for training and test stages outperforms other applied predictive techniques. Therefore, this model introduced in this study can be used in other projects using TBMs for predicting their performances. By conducting the sensitivity analysis, the importance score of each input variable was obtained using the MI technique. The results of 1.4513, 1.2889, 1.0402, 0.9455, 0.9441, 0.8780, and 0.0572 were achieved as importance score of TFC, RPM, RMR, UCS, RQD, BTS, and WZ, respectively, which confirmed that TFC, RPM and RMR variables are considered as highly sensitive factors on TBM AR. However, it should be noted that more data and analysis are needed to consider the TBM operation under other extreme conditions. Therefore, the application of the hybrid model proposed in this paper is only recommended under similar conditions and within a reasonable range of database information. In the future, an extended experimental database with more samples and features should be used to improve the predictive ability of the model. Moreover, the artificial-intelligence-based techniques cannot completely replace traditional effective methods. In terms of geotechnical engineering, the future development direction of AI technology is a composite system, which only develops towards decision support tools. Notably, the smart methods used are only recommended to be applied under similar conditions in this study. The main limitation of such techniques in geotechnical field can be referred to site specific data used in proposing AI models. The geological and geotechnical data and observations can be different from site to site and distance to distance and due to that generalizations of the proposed AI models is a difficult task.

CRediT authorship contribution statement

Jian Zhou: Conceptualization, Methodology, Resources, Validation, Software, Investigation, Visualization, Writing- review & editing, Supervision. **Yingui Qiu:** Validation, Formal analysis, Visualization, Software, Data curation, Writing- original draft. **Shuangli Zhu:** Validation, Formal analysis, Visualization. **Danial Jahed Armaghani:** Resources, Investigation, Writing- review & editing, Supervision. **Chuanqi Li:** Formal analysis, Visualization. **Hoang Nguyen:** Formal analysis, Writing-review & editing, Supervision. **Saffet Yagiz:** Validation, Writing- review & editing.

Declaration of competing interest

The authors declare that they have no known competing financial interests or personal relationships that could have appeared to influence the work reported in this paper.

Acknowledgments

This research was funded by the National Science Foundation of China (41807259), and the Innovation-Driven Project of Central South University (2020CX040). Additionally, the authors wish to express their appreciation to the Universiti Teknologi Malaysia (UTM) for supporting this study during data collection stage. Additionally, the authors wish to express their appreciation to the Universiti Teknologi Malaysia (UTM) for supporting this study during data collection stage.

References

Abderazek, H., Yildiz, A.R., Mirjalili, S., 2020. Comparison of recent optimization algorithms for design optimization of a cam-follower mechanism. Knowl.-Based Syst. 191, 105237.

Adoko, A.C., Gokceoglu, C., Yagiz, S., 2017. Bayesian prediction of TBM penetration rate in rock mass. Eng. Geol. 226, 245–256.

Altan, A., Hacıoğlu, R., 2020. Model predictive control of three-axis gimbal system mounted on UAV for real-time target tracking under external disturbances. Mech. Syst. Signal Process. 138, 106548.

Altan, A., Karasu, S., Bekiros, S., 2019. Digital currency forecasting with chaotic meta-heuristic bio-inspired signal processing techniques. Chaos Solitons Fractals 126, 325–336.

Alvarez Grima, M., Bruines, P.A., Verhoef, P.N.W., 2000. Modeling tunnel boring machine performance by neuro-fuzzy methods. Tunn. Undergr. Space Technol. 15 (3), 259–269.

Alvarez Grima, M., Verhoef, P.N.W., 1999. Forecasting rock trencher performance using fuzzy logic. Int. J. Rock Mech. Min. Sci. 36 (4), 413–432.

Armaghani, D.J., Faradonbeh, R.S., Momeni, E., Fahimifar, A., Tahir, M.M., 2018. Performance prediction of tunnel boring machine through developing a gene expression programming equation. Eng. Comput. 34 (1), 129–141.

Armaghani, D.J., Hajihassani, M., Bejarbaneh, B.Y., Marto, A., Mohamad, E.T., 2014. Indirect measure of shale shear strength parameters by means of rock index tests through an optimized artificial neural network. Measurement 55, 487–498.

Armaghani, D.J., Koopialipoor, M., Marto, A., Yagiz, S., 2019. Application of several optimization techniques for estimating TBM advance rate in granitic rocks. J. Rock Mech. Geotech. Eng. 11 (4), 779–789.

Armaghani, D.J., Mohamad, E.T., Narayanasamy, M.S., Narita, N., Yagiz, S., 2017. Development of hybrid intelligent models for predicting TBM penetration rate in hard rock condition. Tunn. Undergr. Space Technol. 63, 29–43.

Armaghani, D.J., Momeni, E., 2015. Feasibility of ANFIS model for prediction of ground vibrations resulting from quarry blasting. Environ. Earth Sci. 74 (4), 2845–2860.

Bamford, W.F., 1984. Rock test indices are being successfully correlated with tunnel boring machine performance. In: Proceedings of the 5th Australian Tunneling Conference, Melbourne. pp. 9–22.

Banan, A., Nasiri, A., Taheri-Garavand, A., 2020. Deep learning-based appearance features extraction for automated carp species identification. Aquac. Eng. 89, 102053.

Barton, N., 2000. TBM Tunnelling in Jointed and Faulted Rock. Balkema, Rotterdam.

Benardos, A.G., Kaliampakos, D.C., 2004. Modelling TBM performance with artificial neural networks. Tunn. Undergr. Space Technol. 19 (6), 597–605.

Benato, A., Oreste, P., 2015. Prediction of penetration per revolution in tbm tunneling as a function of intact rock and rock mass characteristics. Int. J. Rock Mech. Min. Sci. 74, 119–127.

Bieniawski, Z.T., Caleda, B., Galera, J.M., Alvares, M.H., 2006. Rock mass excavability (RME) index. In: ITA World Tunnel Congress (Paper No. PITA06-254), April, Seoul.

Bruines, P., 1998. Neuro-fuzzy modeling of TBM performance with emphasis on the penetration rate. In: Memoirs of the Centre of Engineering Geology in the Netherlands, Delft, No. 173. p. 202, ISSN 1386-5072.

Bruland, A., 1998. Hard Rock Tunnel Boring (Ph.D. Thesis). Norwegian University of Science and Technology, Trondheim.

Bui, X.N., Nguyen, H., Choi, Y., Nguyen-Thoi, T., Zhou, J., Dou, J., 2020. Prediction of slope failure in open-pit mines using a novel hybrid artificial intelligence model based on decision tree and evolution algorithm. Sci. Rep. 10 (1), 1–17.

Bunawan, A.R., Momeni, E., Armaghani, D.J., Rashid, A.S.A., 2018. Experimental and intelligent techniques to estimate bearing capacity of cohesive soft soils reinforced with soil-cement columns. Measurement 124, 529–538.

Ceryan, N., Okkan, U., Samui, P., Ceryan, S., 2013. Modeling of tensile strength of rocks materials based on support vector machines approaches. Int. J. Numer. Anal. Methods Geomech. 37 (16), 2655–2670.

Champasak, P., Panagant, N., et al., 2020. Self-adaptive many-objective meta-heuristic based on decomposition for many-objective conceptual design of a fixed wing unmanned aerial vehicle. Aerosp. Sci. Technol. 100, 105783.

Cherkassky, V., Ma, Y., 2004. Practical selection of SVM parameters and noise estimation for SVM regression. Neural Netw. 17 (1), 113–126.

Ding, Z., Nguyen, H., Bui, X.N., Zhou, J., Moayedi, H., 2020. Computational intelligence model for estimating intensity of blast-induced ground vibration in a mine based on imperialist competitive and extreme gradient boosting algorithms. Nat. Resour. Res. 29, 751–769.

Eftekhari, M., Baghbanan, A., Bayati, M., 2010. Predicting penetration rate of a tunnel boring machine using artificial neural network. In: ISRM International Symposium–6th Asian Rock Mechanics Symposium. International Society for Rock Mechanics. pp. 1–7.

Faizollahzadeh Ardabili, S., Najafi, B., Shamshirband, S., Minaei Bidgoli, B., Deo, R.C., Chau, K.W., 2018. Computational intelligence approach for modeling hydrogen production: A review. Eng. Appl. Comput. Fluid Mech. 12 (1), 438–458.

Fan, Y., Xu, K., Wu, H., Zheng, Y., Tao, B., 2020. Spatiotemporal modeling for nonlinear distributed thermal processes based on KL Decomposition, MLP and LSTM Network. IEEE Access 8, 25111–25121.

Farfani, H.A., Behnamfar, F., Fathollahi, A., 2015. Dynamic analysis of soil–structure interaction using the neural networks and the support vector machines. Expert Syst. Appl. 42 (22), 8971–8981.

Farrokh, E., Rostami, J., Laughton, C., 2012. Study of various models for estimation of penetration rate of hard rock TBMs. Tunn. Undergr. Space Technol. 30, 110–123.

Fattahi, H., 2016. Adaptive neuro fuzzy inference system based on fuzzy C–means clustering algorithm, A technique for estimation of TBM penetration rate. Iran Univ. Sci. Technol. 6 (2), 159–171.

Frough, O., Torabi, S.R., Yagiz, S., 2015. Application of RMR for estimating rockmass–related TBM utilization and performance parameters: A case study. Rock Mech. Rock Eng. 48 (3), 1305–1312.

Gao, B., Wang, R., Lin, C., Guo, X., Liu, B., Zhang, W., 2020. TBM penetration rate prediction based on the long short-term memory neural network. Undergr. Space http://dx.doi.org/10.1016/j.undsp.2020.01.003.

Ghasemi, E., Yagiz, S., Ataei, M., 2014. Predicting penetration rate of hard rock tunnel boring machine using fuzzy logic. Bull. Eng. Geol. Environ. 73 (1), 23–35.

Gholami, M., Shahriar, K., Sharifzadeh, M., Hamidi, J.K., 2012. A comparison of artificial neural network and multiple regression analysis in tbm performance prediction. In: ISRM Regional Symposium–7th Asian Rock Mechanics Symposium. International Society for Rock Mechanics.

Gholamnejad, J., Tayarani, N., 2010. Application of artificial neural networks to the prediction of tunnel boring machine penetration rate. Min. Sci. Technol. (China) 20 (5), 727–733.

Gong, Q.M., Zhao, J., 2009. Development of a rock mass characteristics model for TBM penetration rate prediction. Int. J. Rock Mech. Min. Sci. 46 (1), 8–18.

Graham, P.C., 1976. Rock exploration for machine manufacturers. In: Bieniawski, Z.T. (Ed.), Exploration for Rock Engineering. Balkema, Johannesburg, pp. 173–180.

Grima, M.A., Bruines, P.A., Verhoef, P.N.W., 2000. Modeling tunnel boring machine performance by neuro-fuzzy methods. Tunn. Undergr. Space Technol. 15 (3), 259–269.

Gunn, S.R., 1998. Support vector machines for classification and regression. ISIS Tech. Rep. 14 (1), 5–16.

Guo, H., Zhou, J., Koopialipoor, M., Armaghani, D.J., Tahir, M.M., 2019. Deep neural network and whale optimization algorithm to assess flyrock induced by blasting. Eng. Comput. 1–14. http://dx.doi.org/10.1007/s00366-019-00816-y.

Hamidi, K.J., Shahriar, K., Rezai, B., Bejari, H., 2010. Application of fuzzy set theory to rock engineering classification systems: an illustration of the rock mass excavability index. Rock Mech. Rock Eng. 43 (3), 335–350.

Hamza, F., Abderazek, H., Lakhdar, S., Ferhat, D., Yıldız, A.R., 2018. Optimum design of cam-roller follower mechanism using a new evolutionary algorithm. Int. J. Adv. Manuf. Technol. 99 (5–8), 1267–1282.

Hassanpour, J., Rostami, J., Zhao, J., 2011. A new hard rock TBM performance prediction model for project planning. Tunn. Undergr. Space Technol. 26, 595–603.

Hu, P., Pan, J.S., Chu, S.C., 2020. Improved Binary Grey Wolf Optimizer and its application for feature selection. Knowl.-Based Syst. 105746.

ISRM, 2007. The complete ISRM suggested methods for rock characterization, testing and monitoring: 1974–2006. In: Ulusay, R., Hudson, J.A. (Eds.), Suggested Methods Prepared by the Commission on Testing Methods. International Society for Rock Mechanics. ISRM Turkish National Group, Ankara, Turkey.

Jahed Armaghani, D., Asteris, P.G., Askarian, B., Hasanipanah, M., Tarinejad, R., Huynh, V.V., 2020. Examining hybrid and single SVM models with different Kernels to predict Rock Brittleness. Sustainability 12 (6), 2229.

Karagöz, S., Yıldız, A.R., 2017. A comparison of recent metaheuristic algorithms for crashworthiness optimisation of vehicle thin-walled tubes considering sheet metal forming effects. Int. J. Veh. Des. 73 (1–3), 179–188.

Karasu, S., Altan, A., 2019. Recognition model for solar Radiation Time Series based on random forest with feature selection approach. In: 2019 11th International Conference on Electrical and Electronics Engineering (ELECO). IEEE, pp. 8–11.

Karasu, S., Altan, A., Sarac, Z., Hacioglu, R., 2017. Prediction of solar radiation based on machine learning methods. J. Cogn. Syst. 2 (1), 16–20.

Karasu, S., Altan, A., Saraç, Z., Hacioğlu, R., 2018. Prediction of Bitcoin prices with machine learning methods using time series data. In: 2018 26th Signal Processing and Communications Applications Conference (SIU). IEEE, pp. 1–4.

Karen, İ., Yildiz, A.R., et al., 2006. Hybrid approach for genetic algorithm and taguchi's method based design optimization in the automotive industry. Int. J. Prod. Res.: Adv. Evol. Comput. Des. Manuf. Probl. 44 (22), 4897–4914.

Khandelwal, M., 2011. Blast-induced ground vibration prediction using support vector machine. Eng. Comput. 27 (3), 193–200.

Khandelwal, M., Singh, T.N., 2009. Prediction of blast-induced ground vibration using artificial neural network. Int. J. Rock Mech. Min. Sci. 46 (7), 1214–1222.

Kiani, M., Yildiz, A.R., 2015. A comparative study of non-traditional methods for vehicle crashworthiness and NVH optimization. Arch. Comput. Methods Eng. 23 (4), 723–734.

Koopialipoor, M., Fahimifar, A., Ghaleini, E.N., Momenzadeh, M., Armaghani, D.J., 2020. Development of a new hybrid ANN for solving a geotechnical problem related to tunnel boring machine performance. Eng. Comput. 36 (1), 345–357.

Koopialipoor, M., Tootoonchi, H., Armaghani, D.J., Mohamad, E.T., Hedayat, A., 2019. Application of deep neural networks in predicting the penetration rate of tunnel boring machines. Bull. Eng. Geol. Environ. 78 (8), 6347–6360.

Kurtuluş, E., Yıldız, A.R., 2020. A novel hybrid harris hawks-simulated annealing algorithm and RBF-based metamodel for design optimization of highway guardrails. Mater. Test. 62 (3), 251–260.

Le, L.T., Nguyen, H., Zhou, J., Dou, J., Moayedi, H., 2019. Estimating the heating load of buildings for smart city planning using a novel artificial intelligence technique PSO-xgboost. Appl. Sci. 9 (13), 2714.

Li, X., Li, X., Su, Y., 2016. A hybrid approach combining uniform design and support vector machine to probabilistic tunnel stability assessment. Struct. Saf. 61, 22–42.

Li, E., Zhou, J., Shi, X., Armaghani, D.J., Yu, Z., Chen, X., Huang, P., 2020. Developing a hybrid model of salp swarm algorithm-based support vector machine to predict the strength of fiber-reinforced cemented paste backfill. Eng. Comput. 1–22.
Liu, B., Wang, R., Zhao, G., Guo, X., Wang, Y., Li, J., Wang, 2020a. Prediction of rock mass parameters in the TBM tunnel based on BP neural network integrated simulated annealing algorithm. Tunn. Undergr. Space Technol. 95, 103103.
Liu, J., Yang, Z., Li, D., 2020b. A multiple search strategies based grey wolf optimizer for solving multi-objective optimization problems. Expert Syst. Appl. 145, 113134.
Mafarja, M.M., Mirjalili, S., 2017. Hybrid whale optimization algorithm with simulated annealing for feature selection. Neurocomputing 260, 302–312.
Mahdevari, S., Shahriar, K., Yagiz, S., Shirazi, M.A., 2014. A support vector regression model for predicting tunnel boring machine penetration rates. Int. J. Rock Mech. Min. Sci. 72, 214–229.
Marto, A., Hajihassani, M., 2014. Bearing capacity of Shallow Foundation's Prediction through hybrid artificial neural networks. Appl. Mech. Mater. 567, 681–686.
Mikaeil, R., Naghadehi, M.Z., Sereshki, F., 2009. Multifactorial fuzzy approach to the penetrability classification of tbm in hard rock conditions. Tunnell. Undergr.Space Technol. 24 (5), 500–505.
Minh, V.T., Katushin, D., Antonov, M., Veinthal, R., 2017. Regression models and fuzzy logic prediction of TBM penetration rate. Open Eng. 7 (1), 60–68.
Mirjalili, S., 2015. Moth-flame optimization algorithm: a novel nature-inspired heuristic paradigm. Knowl.-Based Syst. 89, 228–249.
Mirjalili, S., Lewis, A., 2016. The whale optimization algorithm. Adv. Eng. Softw. 95, 51–67.
Mirjalili, S., Mirjalili, S.M., Lewis, A., 2014. Grey wolf optimizer. Adv. Eng. Softw. 69, 46–61.
Mogana, S.N., 2007. The effects of ground conditions on TBM performance in tunnel excavation – A case history. In: Proceedings of the 10th Australia New Zealand conference on Geomechanics 2007, pp. 442–447.
Mogana, S.N., Rafek, A.G., Komoo, I., 1998. The influence of rock mass properties in the assessment of TBM performance. In: Moore, D., Hungr, O. (Eds.), 8th IAEG Congr. Balkema, Vancouver, Rotterdam, pp. 3553–3559.
Momeni, E., Nazir, R., Armaghani, D.J., Maizir, H., 2014. Prediction of pile bearing capacity using a hybrid genetic algorithm-based ANN. Measurement 57, 122–131.
Momeni, E., Yarivand, A., Dowlatshahi, M.B., Armaghani, D.J., 2020. An efficient optimal neural network based on Gravitational Search Algorithm in predicting the deformation of geogrid-reinforced soil structures. Transp. Geotech. 100446.
Nenavath, H., Jatoth, R.K., Das, S., 2018. A synergy of the sine-cosine algorithm and particle swarm optimizer for improved global optimization and object tracking. Swarm Evol. Comput. 43, 1–30.
Okubo, S., Kfukie, K., Chen, W., 2003. Expert systems for applicability of tunnel boring machine in Japan. Rock Mech. Rock Eng. 36, 305–322.
Oraee, K., Khorami, M.T., Hosseini, N., 2012. Prediction of the penetration rate of tbm using adaptive neuro fuzzy inference system (anfis). In: Proceeding of SME Annual Meeting & Exhibit, From the Mine to the Market, Now It's Global, Seattle, WA, USA. pp. 297–302.
Ozdemir, L., 1977. Development of Theoretical Equations for Predicting Tunnel Borability (Ph.D. Thesis). T-1969, Colorado School of Mines, Golden, CO, USA.
Pal, M., Deswal, S., 2008. Modeling pile capacity using support vector machines and generalized regression neural network. J. Geotech. Geoenviron. Eng. 134 (7), 1021–1024.
Rad, H.N., Hasanipanah, M., Rezaei, M., Eghlim, A.L., 2018. Developing a least squares support vector machine for estimating the blast-induced flyrock. Eng. Comput. 34 (4), 709–717.
Rayatdust, H., Shahriar, K., Ahangari, K., Kamali-Bandpey, H., 2012. A statistical model for prediction TBM performance using rock mass characteristics in the TBM Driven Alborz Tunnel Project. Res. J. Appl. Sci. Eng. Technol. 4 (23), 5048–5054.
Rezaei, H., Nazir, R., Momeni, E., 2016. Bearing capacity of thin-walled shallow foundations: an experimental and artificial intelligence-based study. J. Zhejiang Univ. Sci. A 17, 273–285. http://dx.doi.org/10.1631/jzus.A1500033.
Rostami, J., 1997. Development of a Force Estimation Model for Rock Fragmentation with Disc Cutters Through Theoretical Modeling and Physical Measurement of Crushed Zone Pressure (Ph.D. Thesis). Colorado School of Mines, Golden, Colorado, USA.
Salimi, A., Esmaeili, M., 2013. Utilizing of linear and non–linear prediction tools for evaluation of penetration rate of tunnel boring machine in hard rock condition. Int. J. Min. Miner. Eng. 4 (3), 249–264.
Salimi, Alireza, Rostami, J., Moormann, C., Delisio, A., 2016. Application of non-linear regression analysis and artificial intelligence algorithms for performance prediction of hard rock TBMs. Tunn. Undergr. Space Technol. 58, 236–246.
Samui, P., 2012. Application of statistical learning algorithms to ultimate bearing capacity of shallow foundation on cohesionless soil. Int. J. Numer. Anal. Methods Geomech. 36 (1), 100–110.
Samui, P., Kim, D., 2013. Least square support vector machine and multivariate adaptive regression spline for modeling lateral load capacity of piles. Neural Comput. Appl. 23 (3–4), 1123–1127.
Sapigni, M., Berti, M., Behtaz, E., Busillo, A., Cardone, G., 2002. TBM performance estimation using rock mass classification. Int. J. Rock Mech. Min. Sci. Geomech. Abstr. 39, 771–788.
Saxena, A., Kumar, R., Mirjalili, S., 2020. A harmonic estimator design with evolutionary operators equipped grey wolf optimizer. Expert Syst. Appl. 145, 113–125.
Shamshirband, S., Rabczuk, T., Chau, K.W., 2019. A survey of deep learning techniques: application in wind and solar energy resources. IEEE Access 7, 164650–164666.
Shi, X.Z., Zhou, J., Wu, B.B., Huang, D., Wei, W., 2012. Support vector machines approach to mean block size of rock fragmentation due to bench blasting prediction. Trans. Nonferr. Met. Soc. China 22 (2), 432–441.
Simoes, M.G., Kim, T., 2006. Fuzzy modeling approaches for the prediction of machine utilization in hard rock tunnel boring machines. In: Industry Applications Conference, 2006. 41st IAS Annual Meeting. Conference Record of the 2006 IEEE. IEEE, pp. 947–954.
Snowdon, R.A., Ryley, M.D., Temporal, J., 1982. A study of disc cutting in selected British rocks. Int. J. Rock Mech. Min. Sci. 19, 107–121.
Torabi, S.R., Shirazi, H., Hajali, H., Monjezi, M., 2013. Study of the influence of geotechnical parameters on the tbm performance in tehran–shomal highway project using ann and spss. Arab. J. Geosci. 6 (4), 1215–1227.
Vapnik, V., 1995. The Nature of Statistical Learning Theory. Springer, Berlin.
Verron, S., Tiplica, T., Kobi, A., 2008. Fault detection and identification with a new feature selection based on mutual information. J. Process Control 18 (5), 479–490.
Von Preinl, Z.T., Tamames, B.C., Fernandez, J.M., Hernandez, M.A., 2006. Rock mass excavability indicator: new way to selecting the optimum tunnel construction method. Tunnelling and Underground Space Technology 21 (3–4).
Wang, M., Shi, X., Zhou, J., Qiu, X., 2018. Multi-planar detection optimization algorithm for the interval charging structure of large-diameter longhole blasting design based on rock fragmentation aspects. Eng. Optim. 50 (12), 2177–2191.
Wang, W.C., Xu, L., Chau, K.W., Xu, D.M., 2020. Yin-Yang firefly algorithm based on dimensionally Cauchy mutation. Expert Syst. Appl. 150, 113216.
Wu, C.L., Chau, K.W., 2013. Prediction of rainfall time series using modular soft computing methods. Eng. Appl. Artif. Intell. 26 (3), 997–1007.
Xu, H., Zhou, J., Asteris, P.G., Jahed Armaghani, D., Tahir, M.M., 2019. Supervised machine learning techniques to the prediction of tunnel boring machine penetration rate. Appl. Sci. 9 (18), 3715.
Yagiz, S., 2002. Development of Rock Fracture and Brittleness Indices To Quantifying the Effects of Rock Mass Features and Toughness in the CSM Model Basic Penetration for Hard Rock Tunneling Machines (Ph.D. Thesis). T-5605, Colorado School of Mines, CO, USA.
Yagiz, S., 2008. Utilizing rock mass properties for predicting TBM performance in hard rock conditions. Tunn. Undergr. Space Technol. 23 (3), 326–339.
Yagiz, S., 2017. New equations for predicting the field penetration index of tunnel boring machines in fractured rock mass. Arab. J. Geosci. 10 (2), 33.
Yagiz, S., Gokceoglu, C., Sezer, E., Iplikci, S., 2009. Application of two non-linear prediction tools to the estimation of tunnel boring machine performance. Eng. Appl. Artif. Intell. 22 (4), 808–814.
Yagiz, S., Karahan, H., 2011. Prediction of hard rock TBM penetration rate using particle swarm optimization. Int. J. Rock Mech. Min. Sci. 48 (3), 427–433.
Yagiz, S., Karahan, H., 2015. Application of various optimization techniques and comparison of their performances for predicting TBM penetration rate in rock mass. Int. J. Rock Mech. Min. Sci. 80, 308–315.
Yavari, M., Mahdavi, S., 2005. Prediction of penetration rate of tbm using ann. In: National Mining Conference, 1–3 Feb 2005, Iran. pp. 1–10.
Yildiz, A.R., 2013. Comparison of evolutionary-based optimization algorithms for structural design optimization. Eng. Appl. Artif. Intell. 26 (1), 327–333.
Yildiz, B.S., 2017. A comparative investigation of eight recent population-based optimisation algorithms for mechanical and structural design problems. Int. J. Veh. Des. 73 (1–3), 208–218.
Yildiz, A.R., 2019. A novel hybrid whale–Nelder–Mead algorithm for optimization of design and manufacturing problems. Int. J. Adv. Manuf. Technol. 105 (12), 5091–5104.
Yıldız, B.S., 2020a. Optimal design of automobile structures using moth-flame optimization algorithm and response surface methodology. Mater. Test. 62 (4), 371–377.
Yıldız, B.S., 2020b. The mine blast algorithm for the structural optimization of electrical vehicle components. Mater. Test. 62 (5), 497–501.
Yıldız, B.S., 2020c. The spotted hyena optimization algorithm for weight-reduction of automobile brake components. Mater. Test. 62 (4), 383–388.
Yildiz, A.R., Abderazek, H., et al., 2020a. A comparative study of recent non-traditional methods for mechanical design optimization. Arch. Comput. Methods Eng. 27 (4), 1031–1048.
Yildiz, A.R., Öztürk, F., 2010. Hybrid taguchi-harmony search approach for shape optimization. In: Recent Advances in Harmony Search Algorithm. Springer, Berlin, Heidelberg, pp. 89–98.
Yildiz, B.S., Yildiz, A.R., 2017. Moth-flame optimization algorithm to determine optimal machining parameters in manufacturing processes. Mater. Test. 59 (5), 425–429.
Yildiz, B.S., Yildiz, A.R., 2018. Comparison of grey wolf, whale, water cycle, ant lion and sine-cosine algorithms for the optimization of a vehicle engine connecting rod. Mater. Test. 60, 311–315.
Yıldız, B.S., Yıldız, A.R., 2019. The harris hawks optimization algorithm, salp swarm algorithm, grasshopper optimization algorithm and dragonfly algorithm for structural design optimization of vehicle components. Mater. Test. 61 (8), 744–748.

Yıldız, B.S., Yıldız, A.R., Albak, Abderazek, H., Sait, S.M., Bureerat, S., 2020b. Butterfly optimization algorithm for optimum shape design of automobile suspension components. Mater. Test. 62 (4), 365–370.

Yıldız, B.S., Yıldız, A.R., Pholdee, N., Bureerat, S., Sait, S.M., Patel, V., 2020c. The henry gas solubility optimization algorithm for optimum structural design of automobile brake components. Mater. Test. 62 (3), 261–264.

Yong, W., Zhou, J., Armaghani, D.J., Tahir, M.M., Tarinejad, R., Pham, B.T., Van Huynh, V., 2020. A new hybrid simulated annealing-based genetic programming technique to predict the ultimate bearing capacity of piles. Eng. Comput. 1–17.

Yu, Z., Shi, X., Zhou, J., Chen, X., Miao, X., Teng, B., Ipangelwa, T., 2020b. Prediction of blast-induced rock movement during bench blasting: Use of gray wolf optimizer and support vector regression. Nat. Resour. Res. 29, 843–865.

Yu, Z., Shi, X., Zhou, J., Chen, X., Qiu, X., 2020a. Effective assessment of blast-induced ground vibration using an optimized random forest model based on a harris hawks optimization algorithm. Appl. Sci. 10 (4), 1403.

Yu, Z., Shi, X., Zhou, J., Gou, Y., Huo, X., Zhang, J., Armaghani, D.J., 2020c. A new multikernel relevance vector machine based on the HPSOGWO algorithm for predicting and controlling blast-induced ground vibration. Eng. Comput. 1–16.

Yu, Z., Shi, X., Zhou, J., Rao, D., Chen, X., Dong …, W., Ipangelwa, T., 2019. Feasibility of the indirect determination of blast-induced rock movement based on three new hybrid intelligent models. Eng. Comput. 1–16.

Zhang, W.G., Li, H.R., Wu, C.Z., Li, Y.Q., Liu, Z.Q., Liu, H.L., 2020b. Soft computing approach for prediction of surface settlement induced by earth pressure balance shield tunneling. Undergr. Space http://dx.doi.org/10.1016/j.undsp.2019.12.003.

Zhang, P., Wu, H.N., Chen, R.P., Chan, T.H., 2020a. Hybrid meta-heuristic and machine learning algorithms for tunneling-induced settlement prediction: A comparative study. Tunn. Undergr. Space Technol. 99, 103383.

Zhang, W.G., Zhang, R., Wu, C., Goh, A.T.C., Lacasse, S., Liu, Z., Liu, H., 2020c. State-of-the-art review of soft computing applications in underground excavations. Geosci. Front. 11 (4), 1095–1106.

Zhao, H.B., Yin, S., 2009. Geomechanical parameters identification by particle swarm optimization and support vector machine. Appl. Math. Model. 33 (10), 3997–4012.

Zheng, G., Zhang, W., Zhang, W., Zhou, H., Yang, P., 2020. Neural network and support vector machine models for the prediction of the liquefaction-induced uplift displacement of tunnels. Undergr. Space.

Zhou, J., Asteris, P.G., Armaghani, D.J., Pham, B.T., 2020f. Prediction of ground vibration induced by blasting operations through the use of the Bayesian network and random forest models. Soil Dyn. Earthq. Eng. 139, 106390.

Zhou, J., Bejarbaneh, B.Y., Armaghani, D.J., Tahir, M.M., 2020a. Forecasting of TBM advance rate in hard rock condition based on artificial neural network and genetic programming techniques. Bull. Eng. Geol. Environ. 79, 2069–2084.

Zhou, J., Chen, C., Armaghani, D.J., Ma, S., 2020b. Developing a hybrid model of information entropy and unascertained measurement theory for evaluation of the excavatability in rock mass. Eng. Comput. 1–24. http://dx.doi.org/10.1007/s00366-020-01053-4.

Zhou, C., Ding, L., Zhou, Y., Zhang, H., Skibniewski, M.J., 2019a. Hybrid support vector machine optimization model for prediction of energy consumption of cutter head drives in shield tunneling. J. Comput. Civ. Eng. 33 (3), 04019019.

Zhou, J., Guo, H., Koopialipoor, M., Armaghani, D.J., Tahir, M.M., 2020c. Investigating the effective parameters on the risk levels of rockburst phenomena by developing a hybrid heuristic algorithm. Eng. Comput. 1–16. http://dx.doi.org/10.1007/s00366-019-00908-9.

Zhou, J., Li, C., Arslan, C.A., Hasanipanah, M., Amnieh, H.B., 2019b. Performance evaluation of hybrid FFA-ANFIS and GA-ANFIS models to predict particle size distribution of a muck-pile after blasting. Eng. Comput. 1–10. http://dx.doi.org/10.1007/s00366-019-00822-0.

Zhou, J., Li, E., Gong, F., Wang, M., Qiao, Q., 2018. Development of random forests and Cubist models for predicting TBM penetration rate in hard rock condition. In: The 15th Annual Meeting of Chinese rock mechanics and Engineering (China Rock 2018). Beijing, China. p. 10.

Zhou, J., Li, C., Koopialipoor, M., Jahed Armaghani, D., Thai Pham, B., 2020d. Development of a new methodology for estimating the amount of PPV in surface mines based on prediction and probabilistic models (GEP-MC). Int. J. Min. Reclam. Environ. 1–21.

Zhou, J., Li, X., Mitri, H.S., 2015. Comparative performance of six supervised learning methods for the development of models of hard rock pillar stability prediction. Nat. Hazards 79 (1), 291–316.

Zhou, J., Li, X., Mitri, H.S., 2016. Classification of rockburst in underground projects: Comparison of ten supervised learning methods. J. Comput. Civ. Eng. 30 (5), 04016003.

Zhou, J., Li, X.B., Shi, X.Z., 2012. Long-term prediction model of rockburst in underground openings using heuristic algorithms and support vector machines. Saf. Sci. 50 (4), 629–644.

Zhou, J., Li, E.M., Wang, M., Chen, X., Shi, X., Jiang, L., 2019c. Feasibility of stochastic gradient boosting approach for evaluating seismic liquefaction potential based on SPT and CPT case histories. J. Perform. Constr. Facil. 33 (3), 04019024.

Zhou, J., Li, E., Wei, H., Li, C., Qiao, Q., Armaghani, D.J., 2019e. Random forests and cubist algorithms for predicting shear strengths of rockfill materials. Appl. Sci. 9 (8), 1621.

Zhou, J., Li, E., Yang, S., Wang, M., Shi, X., Yao, S., Mitri, H.S., 2019d. Slope stability prediction for circular mode failure using gradient boosting machine approach based on an updated database of case histories. Saf. Sci. 118, 505–518.

Zhou, J., Qiu, Y., Zhu, S., Armaghani, D.J., Khandelwal, M., Mohamad, E.T., 2020e. Estimation of the TBM advance rate under hard rock conditions using XGBoost and Bayesian optimization. Undergr. Space http://dx.doi.org/10.1016/j.undsp.2020.05.008.

Zhou, J., Shi, X., Du, K., Qiu, X., Li, X., Mitri, H.S., 2017a. Feasibility of random-forest approach for prediction of ground settlements induced by the construction of a shield-driven tunnel. Int. J. Geomech. 17 (6), 04016129.

Zhou, Y., Su, W., Ding, L., Luo, H., Love, P.E., 2017b. Predicting safety risks in deep foundation pits in subway infrastructure projects: support vector machine approach. J. Comput. Civ. Eng. 31 (5), 04017052.

Zhou, T., Zhu, J.B., Ju, Y., Xie, H.P., 2019f. Volumetric fracturing behavior of 3D printed artificial rocks containing single and double 3D internal flaws under static uniaxial compression. Eng. Fract. Mech. 205, 190–204.

Zorlu, K., Gokceoglu, C., et al., 2008. Prediction of uniaxial compressive strength of sandstones using petrography-based models. Eng. Geol. 96 (3–4), 141–158.